Preprints.org

Review

Not peer-reviewed version

Granulation of Lithium-Ion Sieves (LISs) Using Biopolymers: A Review

Inimfon A Udoetok *, Abdalla H Karoyo *, Emmanuel E Ubuo, Edidiong D Asuquo

Posted Date: 6 February 2024

doi: 10.20944/preprints202402.0329.v1

Keywords: Granulation; biopolymer; lithium-ion sieves (LISs); adsorption capacity; crosslinking; mechanical strength

Preprints.org is a free multidiscipline platform providing preprint service that is dedicated to making early versions of research outputs permanently available and citable. Preprints posted at Preprints.org appear in Web of Science, Crossref, Google Scholar, Scilit, Europe PMC.

Copyright: This is an open access article distributed under the Creative Commons Attribution License which permits unrestricted use, distribution, and reproduction in any medium, provided the original work is properly cited.

Preprints.org (www.preprints.org) | NOT PEER-REVIEWED | Posted: 6 February 2024 doi:10.20944/preprints202402.0329.v1

Disclaimer/Publisher's Note: The statements, opinions, and data contained in all publications are solely those of the individual author(s) and contributor(s) and not of MDPI and/or the editor(s). MDPI and/or the editor(s) disclaim responsibility for any injury to people or property resulting from any ideas, methods, instructions, or products referred to in the content.

Review

Granulation of Lithium-Ion Sieves (LISs) Using Biopolymers: A Review

Inimfon A. Udoetok [a,b,*], Abdalla H. Karoyo [c,*], Emmanuel E. Ubuo [d], Edidiong and D. Asuquo [e].

[a] Department of Chemistry and Biochemistry, University of Regina, Regina, SK S4S 0A2, Canada.
[b] Lithium Research Centre, Arizona Lithium, 615 W Elliot Rd, Tempe AZ 85284, USA.
[c] Nortek Data Cooling Center, Research and Development, 1502D Quebec Ave, Saskatoon, SK S7K 1V7, Canada.
[d] Department of Chemistry, Akwa Ibom State University, Mkpat Enin 532111, Akwa Ibom State, Nigeria.
[e] Department of Chemical Engineering, The University of Manchester, M13 9PL, Manchester, The United Kingdom.
* Correspondence: Corresponding authors: *E-mail address:* inimfon.udoetok@usask.ca; abdalla.karoyo@usask.ca.

Abstract: The high demand for lithium (Li) relates to clean renewable storage devices and the advent of electric vehicles (EVs). The extraction of Li ions from aqueous media calls for efficient adsorbent materials with various characteristics, such as good adsorption capacity, good selectivity, easy isolation of the Li-loaded adsorbent, and good recovery of the adsorbed Li ions. The widespread use of metal-based adsorbent materials for Li ions extraction relates to various factors: (i) the ease of preparation via inexpensive and facile templation techniques, (ii) excellent selectivity for Li ions in a matrix, (iii) high recovery of the adsorbed ions, and (iv) good cycling performance of the adsorbents. However, the use of nano-sized metal-based LISs is limited due to challenges associated with isolating the loaded adsorbent material from the aqueous media. Adsorbent granulation process employing various binding agents (e.g., biopolymers, synthetic polymers, and inorganic materials) affords functional particles with modified morphological and surface properties that support easy isolation from the aqueous phase upon adsorption of Li ions. Biomaterials (e.g., chitosan, cellulose, alginate, and agar) are of particular interest because their structural diversity renders them amenable to coordination interactions with metal-based LISs to form 3D microcapsules. The current review highlights recent progress in the use of biopolymer binding agents for the granulation of metal-based LISs, along with various crosslinking strategies employed to improve the mechanical stability of the granules. The study reviews the effects of granulation and crosslinking on adsorption capacity, selectivity, isolation, recovery, cycling performance and the stability of the LISs. Adsorbent granulation using biopolymer binders has been reported to modify the uptake properties of the bio-adsorbent materials to varying degrees, in accordance with the surface and textural properties of the binding agent. The review further highlights the importance of granulation and crosslinking for improving the extraction process of Li ions from aqueous media. This review contributes to manifold areas related to industrial application of LISs, as follows: 1) to highlight recent progress in the granulation and crosslinking of metal-based adsorbents for Li ions recovery, 2) to highlight the advantages, challenges, and knowledge gaps of using biopolymer-based binders for granulation of LISs, and finally, 3) to catalyze further research interest into the use of biopolymer binders and various crosslinking strategies to engineer functional adsorbent materials for application in Li extraction industry. Properly engineered extractants for Li ions are expected to offer various cost benefits in terms of capital expenditure, percent Li recovery, and reduced environmental footprint.

Keywords: granulation; biopolymer; lithium-ion sieves (LISs); adsorption capacity; crosslinking; mechanical strength

1. Introduction

The transition to clean renewable energy storage devices, along with the growing popularity of EVs, has led to massive interest in Li production. Li has other attractive applications in various

© 2024 by the author(s). Distributed under a Creative Commons CC BY license.

Preprints.org (www.preprints.org) | NOT PEER-REVIEWED | Posted: 6 February 2024 doi:10.20944/preprints202402.0329.v1

manufacturing sectors, including non-rechargeable batteries, ceramics, glasses, lubricating greases, electrocatalysis, the medicine, among other uses (Figure 1). The utility of Li in the clean renewable energy sector (e.g., rechargeable batteries) relates to its electrochemical activity and high specific heat capacity [1]. The excellent charge holding capacity of Li and the efficient delivery of the stored power makes this element attractive from an application and commercial perspectives. According to the United States Geological Survey (USGS) [2], natural Li exists in various ores, including continental brines, claystone, geothermal brines, hectorite, oilfield brines, and pegmatites.

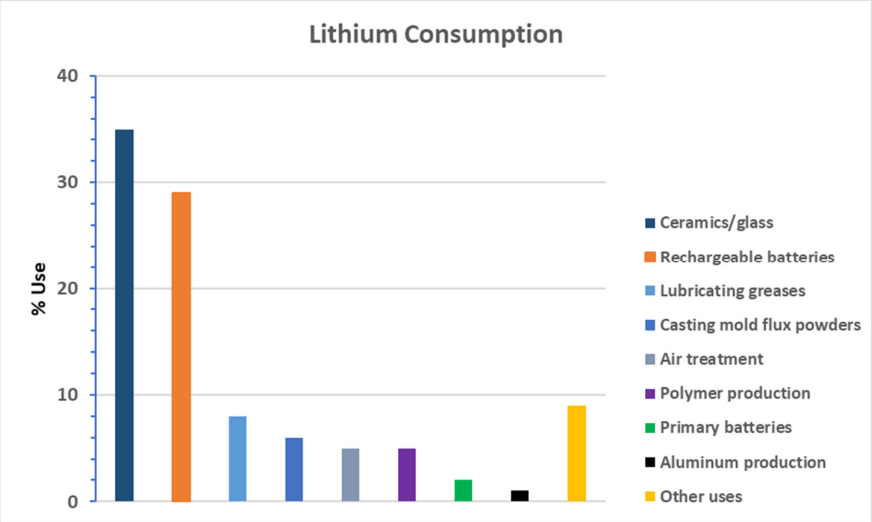

Figure 1. Histogram showing end uses of lithium as a percentage of world consumption. Adapted from Weng at al. [3.].

The global distribution of extractable Li reserves varies as summarized in the pie chart in Figure 2. The bar graph in Figure 2 shows the global consumption of Li for the 2010 – 2020 period, whereas its production is based on existing technologies. It is estimated that the annual demand for elemental Li will increase from 150,000–190,000 tons in 2025 to about 400,000 –700,000 tons in 2100 [4,5]. This high demand, along with the massive natural reserves of Li, suggest that there is a dire need for the development of facile and feasible technologies for its recovery.

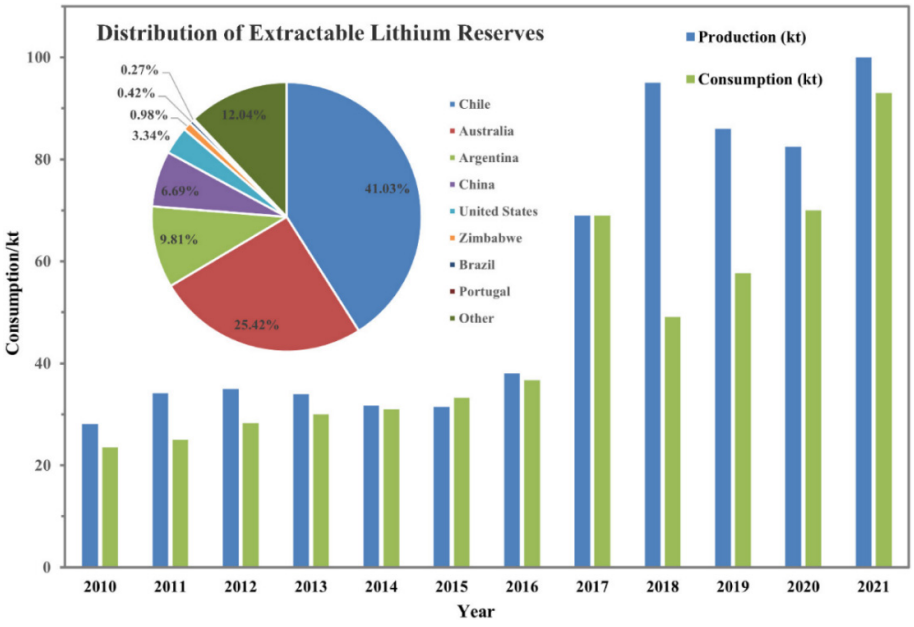

Preprints.org (www.preprints.org) | NOT PEER-REVIEWED | Posted: 6 February 2024 doi:10.20944/preprints202402.0329.v1

Figure 2. Global consumption of Li content from 2010 to 2020 and distribution of extractable Li reserves with existing technologies (reproduced from [6] with copyright permission).

Several technologies for extracting Li ions from aqueous resources exist, such as solar evaporation, chemical precipitation [7,8], solvent extraction [6,9], adsorption [6,10], electrochemical methods [5,6,11], membrane-based technologies [6,12–15], and reaction-coupled separation methods [16–18]. Conventional evaporation-based methods are limited because they are not suitable for processing brine with high magnesium to lithium (Mg/Li) ratios. Additionally, such methods are time consuming and involve complex processes to remove the residual Mg ions [6,19,20]. Similarly, solvent extraction technology is undesirable due to the high cost and toxicity of organic solvents used, along with significant loss of extractant in the aqueous phase [21,22]. Furthermore, poor understanding of the extraction mechanisms suggest that the use of this technique may be subjected to unfavourable outcomes. Adsorption-based technologies are the most feasible and scalable processes due to various advantages: they are simple, efficient, have low carbon footprint, and the adsorbents can recover Li ions at high capacity while rejecting undesired contaminants [6,23–26]. Various organic (e.g., crown ethers and polymer ion-exchange resins) and inorganic (e.g., Al, Mn, and Ti based) materials have been used as adsorbents for Li ions extraction [6,23,25,27,28]. Metal-based adsorbent materials are the most popular due to their relatively lower cost of production, facile synthetic processes, high Li ions recovery, excellent contaminant rejection, and good cycling performance. However, the nano-/micron-sized metal-based adsorbents suffer from poor mechanical strength and challenges associated with isolating the Li-ion loaded adsorbents from the aqueous phase [24].

Granulation of metal-based LISs using biopolymer binding agents has been reported [3,6,24,29] to produce particles with engineered properties such as mechanical strength, porosity, bulk density, and particle size distribution for tailored applications [26,30]. The use of binding agents (e.g., biopolymers, synthetic organic polymers, and inorganic materials) afford LISs that can be easily isolated from the aqueous media, thus enhancing their utility in large scale industrial application. It is worth noting that the granulation of metal-based LISs may be accompanied by reduced uptake properties due to attenuation of accessible binding sites for Li ions adsorption. However, a properly engineered granulation process can ensure that the properties of the LIS granules are optimized in terms of both phase separation and adsorption capacity performances. Moreover, various crosslinking strategies of the LISs prior to and post granulation have been reported to further enhance the mechanical stability of the LIS granules. The current review highlights the recent progress in the use of biopolymer binding agents for the granulation of metal-based adsorbent materials for Li ion extraction. The study further reviews the effects of various biopolymer binding agents on the properties of the granulated materials, such as adsorption capacity, selectivity, isolation, recovery, and cycling performance. Adsorbent granulation process using biopolymer binders has been reported to modify the uptake properties of the bio-adsorbent materials to varying degrees, in accordance with the surface and textural properties of the binding agent. The current study also highlights the importance of granulation technology and various crosslinking strategies for improving the Li ions extraction performance and mechanical properties of the LIS granules, along with their amenability for column operations in large scale industrial application.

2. Preparation of Lithium-Ion Sieves (LIS): An Overview

LISs are generally categorized according to their structural composition, where LMOs (lithium manganese oxides) and LTOs (lithium titanium oxides) are reported as the major classes. The nature and type of the precursors determine the affinity of the LISs for Li ions. Furthermore, the relative ratio of Li and the precursor ion (e.g., Mn or Ti) affects the performance and the regeneration ability of the LISs due to changes in crystallinity. LMO-type LISs, such as λ-MnO_2, $MnO_2{\cdot}0.3H_2O$, and $MnO_2{\cdot}0.5H_2O$, have been synthesized from $LiMn_2O_4$, $Li_{1.33}Mn_{1.67}O_4$ ($Li_4Mn_5O_{12}$), and $Li_{1.6}Mn_{1.6}O_4$ ($Li_2Mn_2O_5$) precursors, with high Li adsorption capacities. Similarly, LTO-type LISs, $H_4Ti_5O_{12}$ and H_2TiO_3, derived from $Li_4Ti_5O_{12}$ and Li_2TiO_3 precursors, have been reported to provide high recovery

Preprints.org (www.preprints.org) | NOT PEER-REVIEWED | Posted: 6 February 2024 doi:10.20944/preprints202402.0329.v1

of Li from aqueous media. Other more complex inorganic precursors have been reported, such as $LiFeMnO_4$, $LiMg_{0.5}Mn_{1.5}O_4$, $LiSbO_3$, $LiAlMnO_4$ and $LiNbO_3$ [31,32]. The reader is referred to an amplitude of references that have reported on the various types of LISs and their preparation strategies [3,6]. The focus in this section is to provide a general strategy for the preparation of LISs.

The preparation of LMO-type LISs will be used as a reference and consists of two steps: (1) preparation of precursors, and (2) acid treatment to intercalate Li ions. The general strategy for the preparation of LISs is depicted in Scheme 1 and is herein described. Several synthetic methods for precursor preparation through Mn and Li templation have been developed. These methods are categorized as solid-phase and soft-chemical methods. In the solid-phase method, Li and Mn salts are mixed according to a certain stoichiometric ratio, followed by calcination at an appropriate temperature to obtain the corresponding products [3,33–36]. Solid-phase methods are simple and easy to apply; however, they suffer from uneven mixing and inadequate reaction of raw materials. By contrast, the soft chemical synthetic method involves the dissolution of Li and Mn compounds in aqueous solutions. Several soft chemical processes, including sol-gel, hydrothermal, and molten-salt techniques have been applied to produce precursors with enhanced homogeneity, purity, and crystallinity. Solid-phase [37,38] and soft chemical methods employing sol-gel [39] and hydrothermal techniques [40,41] are common for precursor preparation in LTO-type LISs. Further details on precursor preparation for LISs can be found in Tables 1–3 and Figure 8 of reference [6]. Upon preparation of precursors, LISs are typically obtained through acid treatment to remove the Li ions (delithiation) while maintaining an imprinted 3D structure. It is worth noting that the Li ion intercalation process may be accompanied by dissolution of Mn, resulting in deformation or possible collapse of the 3D structure. Redox and ion exchange reactions, along with a composite of the two processes, have been reported to be the mechanisms for the intercalation/de-intercalation of Li ions in LISs. Detailed discussions on the acid treatment of precursors and their mechanisms are reported elsewhere [33,42–48]. Crosslinking of biopolymer-based granulated LISs is common [24,49–55] and can be achieved either before or after granulation, with variable outcomes. Crosslinking prior to granulation is anticipated to enhance the integrity of the LIS granules due to the mechanical stability of the crosslinked powdered sieve materials.

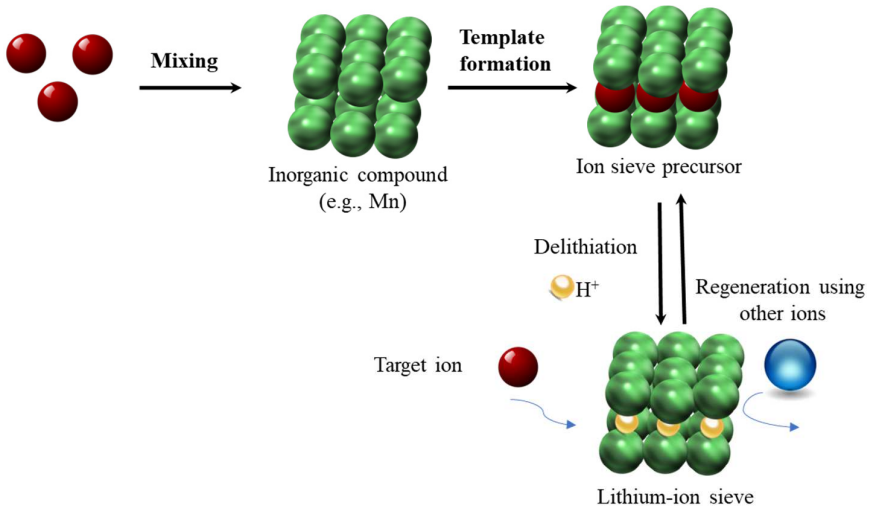

Scheme 1. Schematic representation of the preparation process for lithium ion-sieves.

3. Granulation of LISs

In Section 2, the design of LISs from precursor preparation to intercalation of Li ions by ion exchange using an acid was introduced. This section will focus on the design processes to improve the structural integrity and performance of LISs. Direct Li extraction using nano-based LISs is considered a promising technology for Li recovery since LISs are generally considered non-toxic, cost effective, and chemically stable [56,57]. Moreover, LISs have high capability to selectively extract Li

Preprints.org (www.preprints.org) | NOT PEER-REVIEWED | Posted: 6 February 2024 doi:10.20944/preprints202402.0329.v1

from a matrix that contains other ions like Na, Ca, and Mg. However, since LISs are usually available in powder form, higher pressure drops, and energy consumption impact their Li separation efficiency and limit their use in industrial large-scale applications. Thus, several methods like foaming, granulation, fibre formation, magnetization, and membrane formation have been developed to modify the structure and morphology of LISs to overcome this challenge [58]. Granulation is the generally accepted technology in nanoparticle modification through which LIS powder can form microspheres of various sizes and forms by bonding with the polymeric binding agents. The granulation of LISs provides good mechanical strength, making the microspheres to easily adapt to industrial column operation. While the current study focuses on biomaterial-based binders, some examples of literature is provided on the use of inorganic particles as binding agents for LISs.

3.1. Granulation of LISs Using Inorganic Materials

Among the binders used for the granulation of metal based LISs, studies that report on the use of synthetic organic polymers and inorganic materials are prevalent in the open literature and will be highlighted here. For example, Xiao et. al. [59], Zhu et. al. [60], and Yang et. al. [61] evaluated the adsorption properties of LISs granulated with polyvinyl chloride (PVC) as the binder. Nisola et. al. [62] have fabricated and evaluated the Li uptake properties of macroporous foam composites made of polyvinyl alcohol (PVA). Similarly, Limjuco and coworkers [63] have prepared H_2TiO_3 composite granules for efficient and continuous recovery of Li ions from liquid resources using PVA as the binder. Xiao et. al. [64] prepared LMO-based granulated sieves with a polyacrylamide (PAM) binder via inverse suspension polymerization method, resulting in microspheres with a diameter range between 0.3–0.7 mm. In another study, Jia and coworkers [65] prepared and evaluated the adsorption-desorption properties of LMO sieves granulated with polyacrylonitrile and polyvinylpyrrolidone binders. Epoxy resins have also been used as binders for granulating LISs and subsequent use for recovering Li ions from brine with good adsorption and recovery performance [59,60]. For instance, Liu et. al. [68] and Zhang et. al. [69] employed an amphiphilic epoxy-based binder (polyvinyl butyral) for granulation of LTO-sieves for the recovery of Li ions from brines of varying pH conditions. The use of mineral-based binders (e.g., alumina and silica) has also been reported in the literature. Hong et al. [23,70] have employed alpha-alumina beads (AABs) and calcined mesoporous alumina (Al_2O_3) as immobilizers/binders to enhance the textural and surface properties of LTO-sieves for efficient recovery of Li ions from brine. The granulated LISs prepared by Hong and coworkers with AAB binder showed excellent Li ion recovery (8.87 mg g^{-1}) from seawater with good cycling performance after up to 15 adsorption-desorption cycles. On the other hand, the LISs granulated from mesoporous alumina exhibited Li ion uptake capacity comparable to that of the corresponding powder material owing to the expanded surface area and porous structure imparted by the mesoporous γ-Al_2O_3 binder (*cf.* Figure 3). However, the use of an excessive amount of Al_2O_3 in the later negatively impacted on the crystallinity of the LMO spinel structure and led to Mn dissolution during the regeneration process. The later highlights the importance of maintaining an optimum ratio of LISs/binder for optimal performance of the granulated LIS adsorbents.

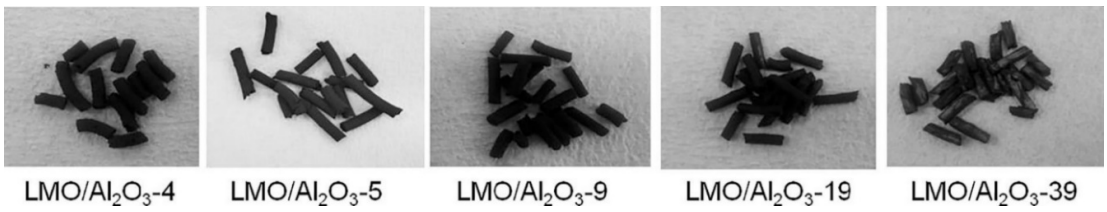

Figure 3. Pictures of LMO/Al2O3 composites (Reproduced from [23] with permissio.n).

Contrary to several reports on the use of organic and inorganic materials as binders for the granulation of metal-based LISs, reports on the use of biopolymers as binders are limited in the open literature (*cf.* Figure 4) [24,49–54,71–79]. Additionally, there are currently no review articles that highlight the available knowledge gaps on the use of biopolymers as binders for the granulation of

Preprints.org (www.preprints.org) | NOT PEER-REVIEWED | Posted: 6 February 2024 doi:10.20944/preprints202402.0329.v1

LISs. Most recent studies have focused on the use of chitosan, alginate, agar, and cellulose as binders to prepare granulated LISs [24,49–54,71–79]. For instance, numerous studies [49–53] have reported on the use of chitosan in various forms (cross-linked and non-cross-linked) as binder for the granulation of LISs. Similarly, other studies [60–67] have reported on the use of cellulose and its derivatives for the granulation of LISs. Li et. al. [74], Koilraj et al. [75] Luo et al. [24] and Park et al. [76] reported on the use of crosslinked alginate for the granulation of Li ion sieves, while Han et al. [78] and Chen et al. [79] reported on the use of agar. The non-availability of many research studies and a review article on the use of biopolymers as binders for the granulation of metal-based LISs highlight the need for a greater understanding of the knowledge gaps and limitations on the use of these abundant, nontoxic, environmentally friendly, and low-cost biomaterials in the Li extraction industry (*cf.* Figure 4). This review therefore intends to highlight the knowledge gaps on the use of biopolymers as binders for the granulation of metal-based LISs and catalyse further research into the use of these environmentally friendly materials in the Li industry. Section 3.2 discusses in detail the preparation of LIS granules using biomaterials as the binding agents.

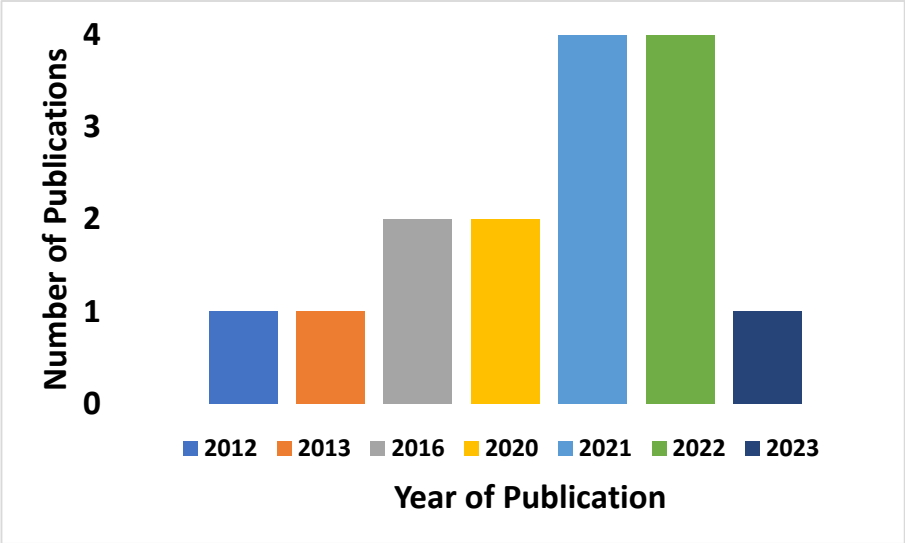

Figure 4. Bar Chart showing the number of publications of granulation of LIS using biopolymers in the last 10 years.

3.2. Granulation of LISs Using Biopolymers

Biopolymers refer to renewable, biodegradable, and environmentally friendly polymers that are derived from animals, plants, and microorganisms [80,81]. They may be classified according to their origin (natural, synthetic, and microbial), and monomer units (e.g., polynucleotides, polypeptides, and polysaccharides) [81]. Biopolymers have gained wide interest in various research fields because of their structural diversity, imparted by the presence of diverse reactive functional groups. Interest for their use in granulation of metal-based LISs relates to their abundance and other unique properties such as non-toxicity, low-cost, and biodegradability with reduced environmental footprint [82]. This review article is focused on the use of chitosan, cellulose, alginate, and agar as binders for the granulation of metal-based LISs. Further details on these selected biopolymers are highlighted below.

3.2.1. Metal-Based LISs Granulated with Chitosan

Chitosan (CTS) is a natural biopolymer derived from chitin, which is found in the exoskeletons of crustaceans, fungi, insects, and some algae [83,84]. The structure of CTS is shown in Figure 5 and comprises of repeating units of glucopyranose rings with amine (-NH_2 or –$NHCOCH_3$) groups at the C-2 unit. The interest in the use of CTS as a binder for the granulation of LISs relates to its good

Preprints.org (www.preprints.org) | NOT PEER-REVIEWED | Posted: 6 February 2024 doi:10.20944/preprints202402.0329.v1

solubility at mildly acidic conditions, low cost, biodegradability, non-toxicity, and its hydrophilic nature.

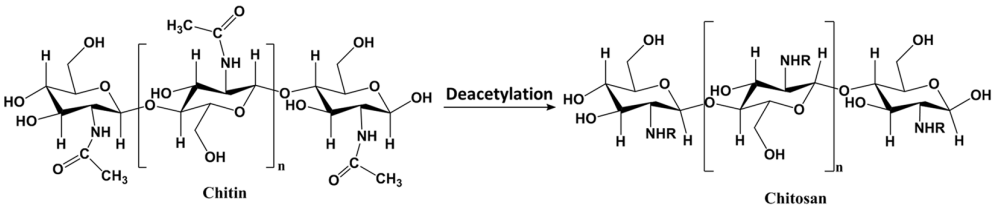

Figure 5. Structure of chitin and chitosan, where n represents the number of repeating units (R = H or acetyl groups according to the level of deacetylation).

Several research groups have reported on the preparation and utility of granulated metal-based LISs using CTS as the binding agent. Hong et al. [49] have prepared mesoporous CTS-granulated LISs using $Li_{1.33}Mn_{1.67}O_4$ precursor, where the precursor was prepared through solid-state synthetic method. The solvation of CTS was achieved by dissolving 6 %wt of the CTS binder in 4% lactic acid at 80 °C. The LMO-based ion sieves (4g) were added to the CTS solution (100 mL) at the 4% (w/v) ratio to form a paste, followed by granulation into cylindrical-shaped microcapsules using an extruder, as depicted in Scheme 2. Delithiation of the prepared granules with 0.2M sulfuric acid revealed a topotactical Li ion extraction at 93% efficiency. Characterization of the prepared granules via FTIR supported the crosslinking of CTS with the sulphate anions (SO_4^{2-}) in sulfuric acid following delithiation. Delithiation of the granules revealed changes in the morphology of the granulated LISs. However, the adsorption capacity of the LIS was retained at ~10 mg/g following the granulation process.

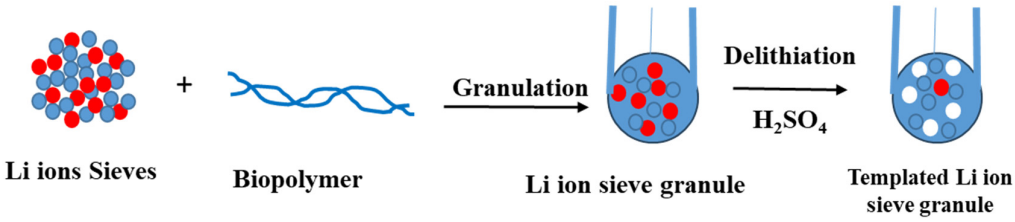

Scheme 2. Granulation of LISs using a Biopolymer Binder.

In another report, Ryu et al. [50] studied the recovery of Li ions from seawater using a continuous flow adsorption column packed with CTS granulated LMO-based microcapsules. The synthetic strategy for the granulated LISs was similar to that reported by Hong and coworkers [49] (*cf.* Scheme 2). The CTS paste was extruded into 0.7nm cylinder-shaped granules, whereas the materials were characterized by FT-IR, where the results agreed with the studies of Hong et al. [49]. Ryu and coworkers evaluated the effects of Li ion concentration, contact time, and recyclability of the prepared CTS-LMO granules. A good Li ion removal efficiency and selectivity was reported, where the adsorption capacity of the granules was recorded at ~54.65 mg/g. The regeneration performance was evaluated using H_2SO_4 (SO_4^{2-}) and revealed a slight decrease in the adsorption capacity of the granules for Li ions after three adsorption-desorption cycles. Similarly, the Li ion recovery capacity decreased slightly from 88 to 85% during the third adsorption-desorption cycle. The trends in the adsorption and recovery capacities were attributed to Mn ion loss (7-9%) and the subsequent collapse of the CTS-LMO granule 3D structure.

In another study, Ding et al. [51] prepared granulated LMO-based LISs, with $Li_4Mn_5O_{12}$ as the precursor, CTS as the binder and a novel crosslinking strategy. The crosslinking strategy employed for the preparation of the granules by Ding et al. [51] is different from the study of Ryu et al. [50] and Hong et al. [49], where sulfate anions were the crosslinking agent. In the present study, the use of

Preprints.org (www.preprints.org) | NOT PEER-REVIEWED | Posted: 6 February 2024 doi:10.20944/preprints202402.0329.v1

epichlorohydrin (ECH) and ethylene glycol diglycidyl ether (EGDE) as crosslinker molecules was aimed at improving the 3D structure and introducing better mechanical strength of the granules that may be lacking in non-crosslinked granulated LISs. The fabrication of the crosslinked LMO LISs is schematically presented in Figure 6. Crosslinking of the LMO sieves using ECH as crosslinker was performed in two steps both prior to- and post-granulation as follows: 3.0 g of the LISs were added to a 3.0 wt% CTS solution in a glacial acetic acid solution and mixed thoroughly. The ECH crosslinker molecule was added in-situ at equimolar concentration with respect to CTS and the mixture was allowed to react for 2 h at 323K. This was followed by slowly dropping the dark brown suspension into a 1M NaOH solution to form spherical granules and the reaction was allowed to continue at 323 K for another 5 h for a second-step cross-linking. The formed spherical adsorbents were washed with ethanol and deionized water in sequence before use. For the EDGE crosslinked granules, 3.00 g of LISs were dispersed in 100 ml of 3.0% CTS. The mixed solution was then dripped into 1 mol/L NaOH to form spherical CTS-LIS granules. After washing to neutral pH, these materials were placed in 100 ml deionized water and the crosslinking with EDGE at mass ratio of EDGE/CTS =2 was carried out at 318 K for 9 h.

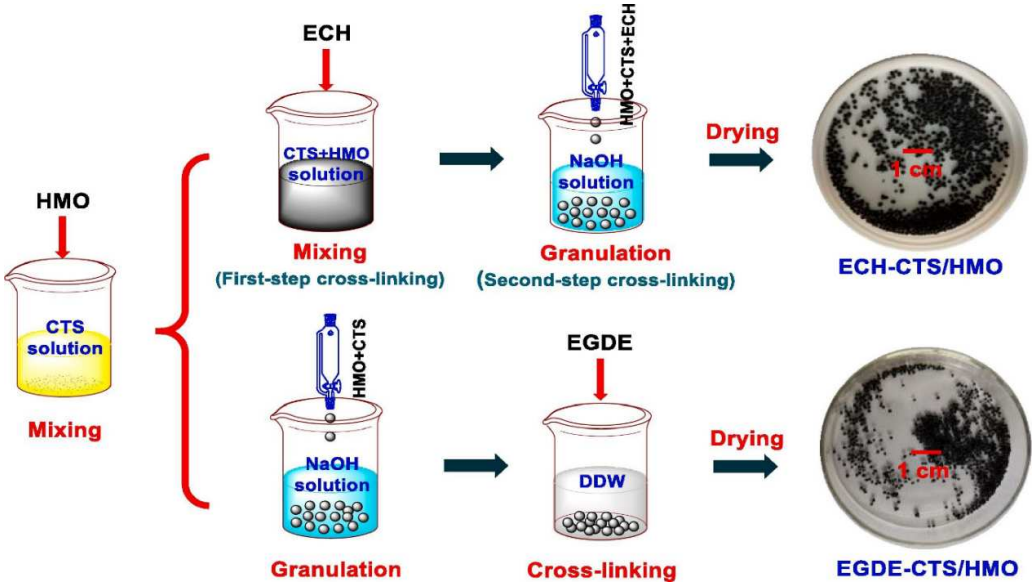

Figure 6. Fabrication of ECH-CTS/HMO and its difference from the preparation of EGDE-CTS/HMO (Reproduced from [51] with permission).

Characterization results reveal a difference in the total organic carbon content of the crosslinked versus non crosslinked granules, where an ECH/CTS ratio of 1:1 was affirmed as the stoichiometric ratio for the reaction. In another study [85], the non-delithiated LISs were observed to agglomerate during the granulation process, thereby not giving room for the preparation of homogenous granules. The agglomeration was affirmed by SEM and particle size analysis results. The authors reported that mass loss due Mn dissolution as well as the adsorption capacity of the granules increased with increasing LISs content, where the ECH crosslinked granule displayed higher Mn dissolution, relative to the EDGE crosslinked granule. TG curves of the ECH and EDGE crosslinked granules revealed that both materials had high chemical stability. The later supports the successful crosslinking of the LIS granules with a concomitant decrease of hydrophilicity relative to pristine CTS, in agreement with contact angle results. Adsorption studies with the granulated LISs revealed that the two-step ECH crosslinked granules display superior adsorption/desorption characteristics relative to the EDGE crosslinked granules (cross-linked after granulation). Due to this reason, the ECH crosslinked material was used for further studies. Adsorption studies with the ECH crosslinked granule reveals that the adsorption capacity increased sharply initially and was 11.40 mg/g after 48

Preprints.org (www.preprints.org) | NOT PEER-REVIEWED | Posted: 6 February 2024 doi:10.20944/preprints202402.0329.v1

h, where the maximum adsorption capacity according to the Langmuir adsorption model was 12.13mg/g, as shown in Figure 7. The Li ion recovery rate was approximated at 88% based on the use of 1g of LISs per 250 mL of a liquid. When the granulated material was further used for Li ion recovery from geothermal water at a solid-to-liquid ratio of 4 g/L, the adsorption capacity and recovery rate were 11.4 mg/g and 88.42%, respectively. The authors also reported that the ECH crosslinked granules revealed a very minimal adsorption capacity loss after 6 adsorption-desorption cycles (Figure 7d), as well as high selectivity for Li-ions in the presence of other contaminants (Figure 7c), where the separation factor between Li and all other ions was greater than 270 (*cf.* Figure 7). This study demonstrates that cross-linking of the biopolymer before granulation leads to greater mechanical and chemical stability.

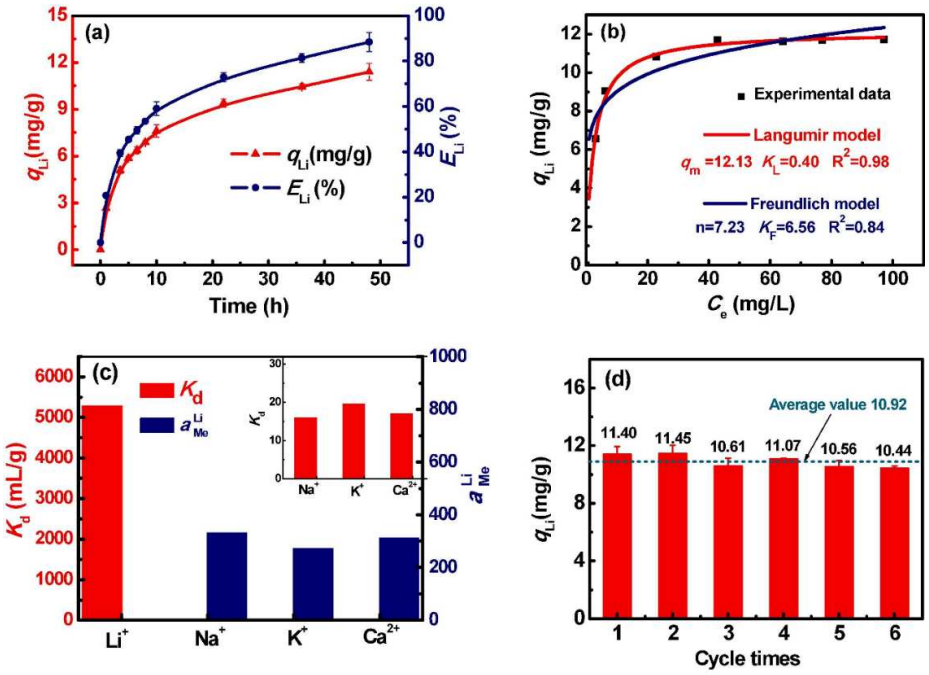

Figure 7. Recovery of Li ion from geothermal water by ECH-CTS/HMO: (a) Variations of adsorption capacity and recovery rate with time (S/L = 1 g/250 mL, pH = 12, T = 333 K); (b) Adsorption isotherms and fitted curves with different isotherm models; (c) Adsorption selectivity; (d) Cyclic stability (Reproduced from [51] with permission).

Yüksel Özşen and Kahvecioğlu [52] have studied the recovery of Li ions from water resources using LMO based LISs granulated with CTS, followed by crosslinking with ECH to enhance their adsorption yield, stability, and reusability. The granulated LISs were prepared using a 3% CTS solution in 2% acetic acid. 2 g of the LISs were added to CTS solution with mixing until a homogenous mixture was obtained, where the CTS-LISs mixture was extruded into a 1 M NaOH solution to obtain the CTS-LIS granules (*cf.* Figure 8). Contrary to the strategy employed by Ding et. al. [66], the crosslinking of the LISs prepared by Yüksel Özşen and Kahvecioğlu [52] was achieved in the presence of NaCl and KOH. It is believed that the role of the salts is to maintain the structural integrity of the beads by modulating their interaction with water through "salting out" effect in agreement with the study of Qilei Zhang et. al. [86]. 5 grams of the granules and 0.075 g of NaCl were added to 75 ml of water containing 0.35 ml of ECH with continuous mixing. This was followed by the slow addition of 2 mL pure water containing 0.3 g of KOH, and the mixture was stirred for 16 hours at 25 °C. The resulting granules were dried at 70 °C for overnight, followed by characterization via SEM, XRD and BET studies. The SEM results show that the granulated adsorbent was mesoporous with the LISs uniformly distributed in the binder matrix. Adsorption studies revealed that the optimum conditions for Li ion uptake by the granulated LISs was pH 12, dosage of 4 g/L and an equilibrium time of 10

Preprints.org (www.preprints.org) | NOT PEER-REVIEWED | Posted: 6 February 2024 doi:10.20944/preprints202402.0329.v1

hours. The Li removal efficiency during the first adsorption cycle was 90% while recovery was 95%. However, during the second cycle, the Li removal efficiency and recovery decreased by 80% and 50%, respectively. The authors attributed the efficiency drop to structural deformity of the granulated materials upon treatment with HCl during delithiation process. The later was affirmed by a decrease in size of the granulated LISs. The granules prepared by Yüksel Özşen and Kahvecioğlu [52] were less stable compared to similar materials prepared Ding et al. [51]. This difference in stability is due to differences in the crosslinking strategies. Crosslinking prior to granulation is anticipated to produce granules with improved mechanical stability in accordance with the results of Ding et al. [51].

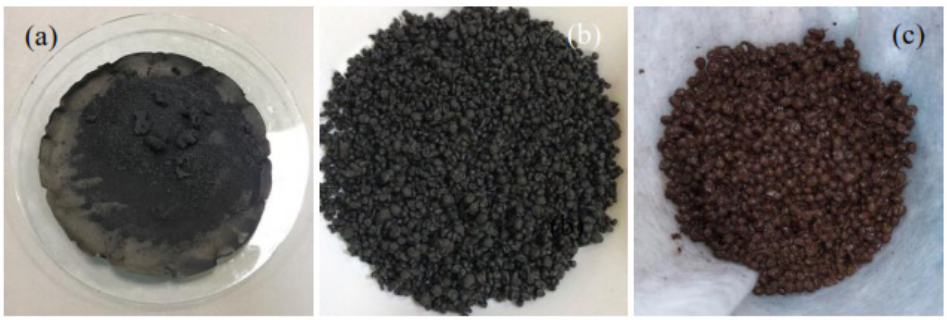

Figure 8. Three forms of adsorbents; a) LMO before granulation with chitosan, b) granulated LMO, c) delithiated LMO (Reproduced from [52] with permission).

Wang et al. [53] granulated different types of LMO sieves, such as $LiMn_2O_4$, $Li_{1.66}Mn_{1.66}O_4$, and $Li_4Mn_5O_{12}$ using CTS as the binder at a mass ratio of CTS/LMO = 3:2 for the selective recovery of Li ions from geothermal water. The granules were prepared using a 3% CTS solution in 2% acetic acid. 2 g of the LMO were added to CTS solution with stirring until a homogenous mixture was obtained. The homogenous mixture was extruded into a 1 M NaOH solution to form the LIS granules. The authors noted that the hydrophilicity of CTS enhanced its hydration in acidic media, thus resulting in the degradation of CTS domain of the granules through dissolution. Crosslinking was carried out post-granulation using various crosslinkers, where the mass ratios were as follows: EDGE/CTS = 2, glutaraldehyde/CTS = 2 and ECH/CTS = 1, and it successfully resolved the degradation of the CTS domain of the granules. Crosslinking has been reported to increase the thermal and chemical stability of biopolymers [80,87,88]. Crosslinking of the granulated LISs with EDGE resulted in reduced CTS mass loss due to dissolution from 27.65% to 0.6%. The authors compared the effects of crosslinking with other crosslinkers such as ECH and GLY and reported that crosslinking with EDGE improved the mechanical and chemical stability of the granules as shown by greater resistance to mass loss due CTS dissolution. Studies on optimization of adsorption and desorption conditions using the granulated LIS reveal that though increase in hydrogen ion concentration and temperature increased the desorption efficiency of the granulated LISs, it negatively impacted on chemical and mechanical stability. Therefore, the optimum conditions for the adsorption process were pH=12 and room temperature, while 0.25 M HCl was most suitable for the desorption process. The authors applied the obtained optimum conditions for the adsorption of Li ions from geothermal water and reported that adsorption equilibrium was attained within 24 h, where the equilibrium adsorption capacity was 8.98 mg/g, as shown in Figure 9. The authors also reported a 1.1% loss in adsorption capacity after 5 adsorption-desorption cycles, where the selectivity coefficient (K_d) for Li ions was 1113.27 mL/g, suggesting high selectivity for Li ions by the granulated LIS materials (*cf.* Figure 9). Contrary to the results of Wang et. al. [67], the greater stability of the ECH-crosslinked granules reported by Ding et al. [51] is accounted for by the use of two-step crosslinking strategy, where cross-linking was performed before and after the granulation process. Despite the use of NaCl and KOH by Yüksel Özşen and Kahvecioğlu [52], the produced LIS granules did not yield LIS materials with better

Preprints.org (www.preprints.org) | NOT PEER-REVIEWED | Posted: 6 February 2024 doi:10.20944/preprints202402.0329.v1

stability relative to materials produced by Ding et al. [51]. The later highlights the importance and effectiveness of introducing crosslinking prior to the granulation process in supporting the chemical and mechanical stability of granulated LISs.

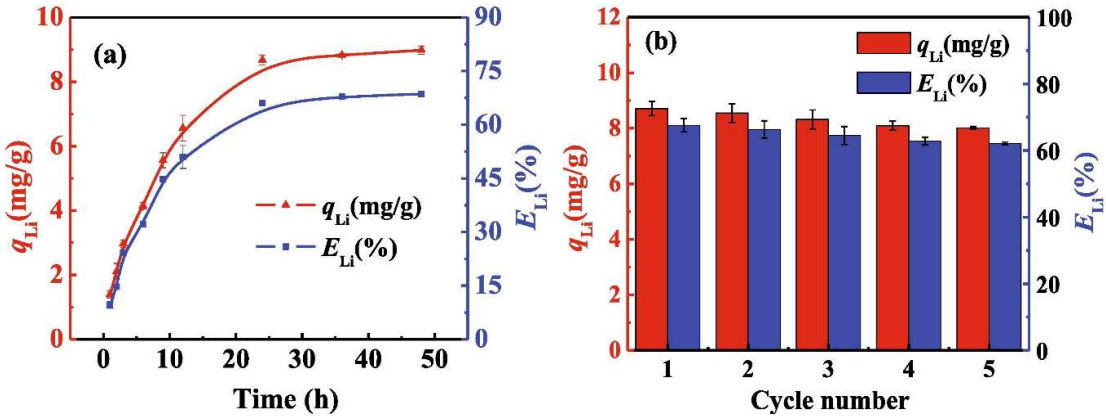

Figure 9. Adsorption of Li ion from geothermal water by cross-linked CTS/HMO at a solid-to-liquid ratio of 1:200 and pH 12. (a) Variations of adsorption capacity and efficiency with time; (b) Cycle stability. (Reproduced from [53] with permission).

3.2.2. Metal-Based LISs Granulated with Cellulose

Cellulose (CLS) (*cf.* Figure 10) is an abundant, environmentally friendly, and renewable biopolymer [80,89,90]. It may be derived from both plants and animals and just like CTS, is composed of D-anhydro glucose units linked by β-l, 4-glucosidic bonds that exist between the carbon atoms C1 and C4 of adjacent glucose units. The only difference between CTS and CLS is the functionality at C-2 of the anhydro glucose unit. The inherent intra/intermolecular hydrogen bond networks of CLS biopolymer affords the formation of partially crystalline and amorphous regions which limits its solubility [91]. However, studies [71,88,92] has shown that the use of mixed solvent systems ranging from alkali/urea solutions [93–95] to ionic liquids (ILs) [96–98] affords the preparation of CLS hydrogels for various industrial applications. Similarly, the synthesis of various derivatives of CLS such as carboxymethyl CLS and hydroxyethyl CLS improves its hydration properties, thus enhancing their solubility in conventional solvents. The interest on the use CLS as green matrices in various applications is related to its hydrophilicity, degradability, and amenability [99]. This section of the review highlights progress in the application of CLS and its derivatives as binders for the granulation of LISs.

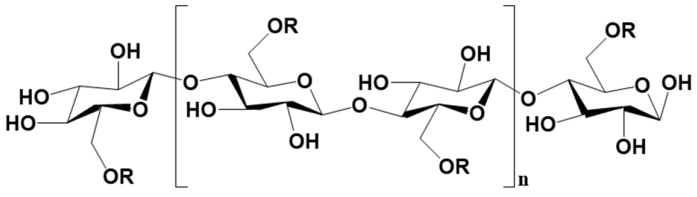

Figure 10. Molecular structure of cellulose, carboxymethyl cellulose and hydroxyethyl cellulose (where n represents the number of repeating units, R = H for cellulose, -CH_2COONa for carboxymethyl cellulose and CH_2CH_2OH for hydroxyethyl cellulose).

Qian et al. [71] developed a series of H_2TiO_3/CLS aerogels (HTO/CA) with a porous network for the selective recovery of Li ions from seawater. The granules were prepared by dissolving CLS in an ionic liquid [Bmim]Cl at 90 °C for 1 h. Subsequently, the LIS (HTO)-CLS mixture with variable CLS to HTO ratio (4:0, 4:1, 4:2, and 4:3) were prepared and thoroughly mixed to afford homogeneity of

Preprints.org (www.preprints.org) | NOT PEER-REVIEWED | Posted: 6 February 2024 doi:10.20944/preprints202402.0329.v1

the mixture. The resulting mixture was poured into a mold, air bubbles removed with the aid of vacuum drying oven, followed by coagulation in an ethanol bath for 24 h. The obtained hydrogel was washed with deionized water, pre-frozen at -12 °C and finally freeze dried under high vacuum conditions for 48 h. The HTO/CA sorbents were characterized using FTIR, XRD, SEM-EDS, contact angle and nitrogen adsorption studies. Nitrogen adsorption results revealed a higher surface area for the HTO/CA (60.38 ± 2.65 m^2/g) relative to HTO powder (22.77 m^2/g), while XRD results noted similar diffraction patterns for HTO powder and HTO/CA [38,39,63] but decreased peak intensities for HTO/CA. The adsorption capacities of the aerogels with different HTO/CA mass ratios were tested and it was observed that the adsorption capacity increased slowly with increase in the loading of HTO powder as shown in Figure 11. The LIS aerogel with the highest HTO loading level (4:4) exhibited a slightly higher adsorption capacity of 28.58 ± 0.71 mg/g relative to the aerogels with other loading levels. The results show that following granulation, this HTO/CA material retained > 90% of the adsorption capacity of the HTO powder (*cf.* Figure 11). Further adsorption studies revealed that HTO/CA exhibited a 69.93 ± 0.04% Li removal from seawater with high affinity for Li ions. Regeneration studies using LiCl solution showed that the Li adsorption capacity of HTO/CA changed slightly after the first 5 adsorption-desorption cycles with the final adsorption capacity being 22.95 mg/g.

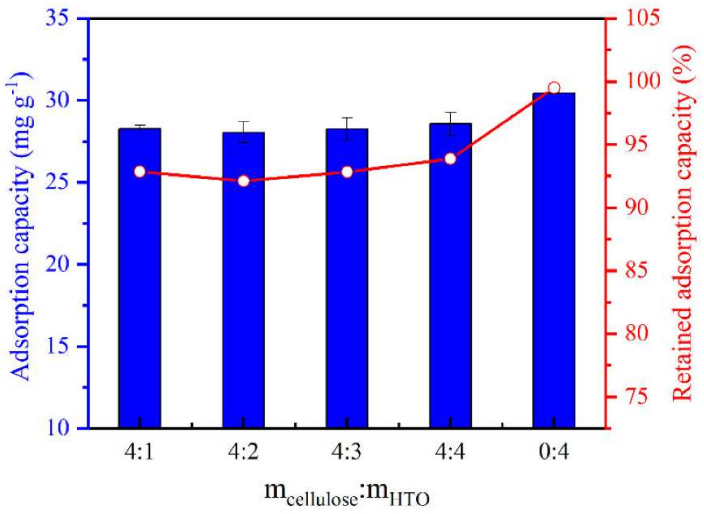

Figure 11. Li ion adsorption capacity of HTO/CA with different HTO loadings and respective % qe retained by HTO in CA for Li+ (pH = 10.25; V = 160 mL; m ≅ 100 mg; C0 = [Li+] ≅ 50 mg L−1). (Reproduced from [71] with permission).

In another study, Xie et al. [54] synthesized spherical composite LISs made of CMC-CLS, EDGE, melamine (ME), and LTO-based sieves with Li_2TiO_3 as the precursor. The multi-step crosslinked granules were made as follows: 1.5 g of Li_2TiO_3, 1.5 g CMC, and 100 mL of double deionized water (DDW) were added to a beaker and stirred at ambient temperature for about 6 h with sonication for several minutes to obtain a homogeneous mixture. The mixture was added dropwise into 100 mL of 2 wt% $FeCl_3$ solution with stirring to obtain the CMC-LTO granules which were washed severally with DDW to remove unreacted chemicals. Crosslinking was achieved by adding the granules to 2 wt% EDGE solution and allowed to react for 6 h at 318.15 K, followed by washing with DDW. The obtained CMC-LTO-EDGE LIS granules were further crosslinked with ME by placing in 2 wt% ME solution and mechanically stirred at 318.15 K for 6 h to afford complete crosslinking reaction (*cf.* Figure 12). The granules were filtered, washed with DDW and dried under vacuum at 318.15 K for 24 h. The synthesized granules were characterized by FTIR and SEM methods. Adsorption studies with the LIS granules showed that optimum conditions for the uptake of Li ions by the granules were: pH 12 and 24 h equilibration time, where the uptake capacity was 12.02 mg/g. Desorption studies at variable concentrations of HCl as the eluent revealed that titanium loss increased with increasing

Preprints.org (www.preprints.org) | NOT PEER-REVIEWED | Posted: 6 February 2024 doi:10.20944/preprints202402.0329.v1

acid concentration. Further studies on the reusability of the LIS granules reveal that there was a marginal decrease in the uptake capacity of LIS granules after each adsorption-desorption cycle. The materials prepared by Xie et al. [54] and Qian et al. [71] offer different strategies to the design of LISs with different adsorption-desorption performance. Xie and coworkers employed the use of a porous aerogel structure to improve the adsorption performance of the LISs. By contrast, Qian et. al. applied a multi-step crosslinking strategy to afford multiple adsorption binding sites, as well as to enhance the mechanical stability of the produced granules.

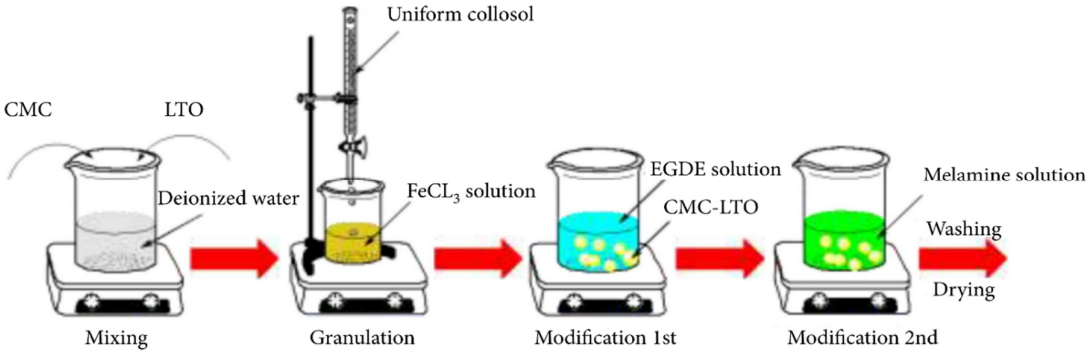

Figure 12. Schematic presentation of CMC-LTO-EGDE-ME microsphere preparation procedure. (Reproduced from [54] with permission).

Zhang et al. [72] reported the preparation of high specific surface LISs templated by bacterial CLS for the selective adsorption of Li ions. The templated LISs were synthesized as follows: Bacterial CLS (B-CLS) hydrogel was added to deionized water for 15 minutes to enhance swelling, followed by freezing with liquid nitrogen and freeze-drying to obtain a B-CLS aerogel network structure. The B-CLS aerogel network was soaked in titanium ethoxide solution for 2 h, rinsed with ethanol and ultrapure water for about four to five times followed by stirring in ultrapure water for 2 h and washed again with deionized water. Finally, the obtained TiO_2/B-CLS material was dried in the oven. The prepared templated LIS was characterized through FTIR, SEM, nitrogen adsorption, and XRD studies. Adsorption studies with the B-CLS templated LISs revealed that uptake was favoured at alkaline pH condition (pH 11), where increasing time favoured the adsorption process till about 200 min. A maximum adsorption capacity of 35.45 mg/g was achieved at equilibrium time of 6 h, which represented 80% of adsorption efficiency. The authors also reported that the B-CLS templated LISs display good selectivity for Li ions as well as strong regeneration ability, where the adsorption capacity remained above 82% of the initial value after 5 adsorption-desorption cycles, as shown in Figure 13. The synthetic strategy employed by Zhang et al. [72] is similar to the study of Qian et al. [71], where the notable difference between the two synthetic strategies relate to the use of an ionic liquid ([Bmim]Cl) for the dissolution of CLS by Qian et al. [71].

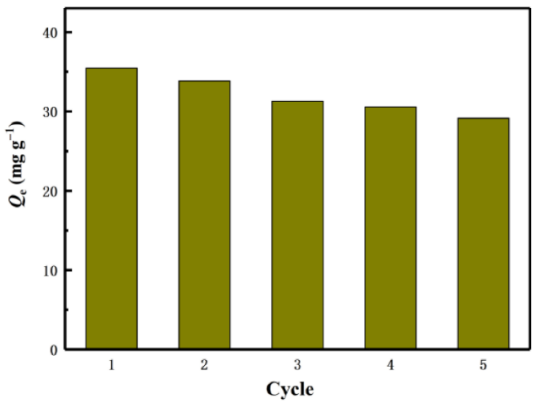

Preprints.org (www.preprints.org) | NOT PEER-REVIEWED | Posted: 6 February 2024 doi:10.20944/preprints202402.0329.v1

Figure 13. Regeneration of H_2TiO_3 five cycles (Reproduced from [72] with permission).

In a separate study, Liu et al. [73] reported on the preparation and characterization of LISs embedded in a hydroxyethyl CLS cryogel (LIS-HEC) for the continuous recovery of Li from brine. The LIS-HEC cryogel was prepared as follows: 1.75 g (3.5% w/w) of HEC and 0.75 g (1.5% w/w) of N, N′-methylenebis (acrylamide) (MBA) were dissolved in deionized water with mixing and sonication to enhance bubbles elimination. Various amounts (0.5, 1.0, 1.5, 2.0, and 2.5 g) of the LISs (LMO) were added to the viscous HEC solution at 0 °C and the resulting mixture stirred for 10 min followed by sonication for 10 min respectively. The stirring and sonication sequence was repeated thrice, followed by the dropwise addition of ammonium persulphate (APS) and 4 wt% N, N, N′, N′ -Tetramethylethylenediamine, (TEMED) solutions to the mixture. The resulting mixture was injected into a cylindrical mold with a 10 mm inner diameter, cooled to -20 °C and held for 24 h. The mixture was thawed at room temperature and rinsed with deionized water to obtain an LMO-HEC cryogel. The LIS-HECs were obtained via treatment of the LMO-HEC with 0.5 M HCl and referred to as LIS-HEC-N, where N in the LIS-HEC-N represents the LIS loading (wt%), as schematically represented in Figure 14.

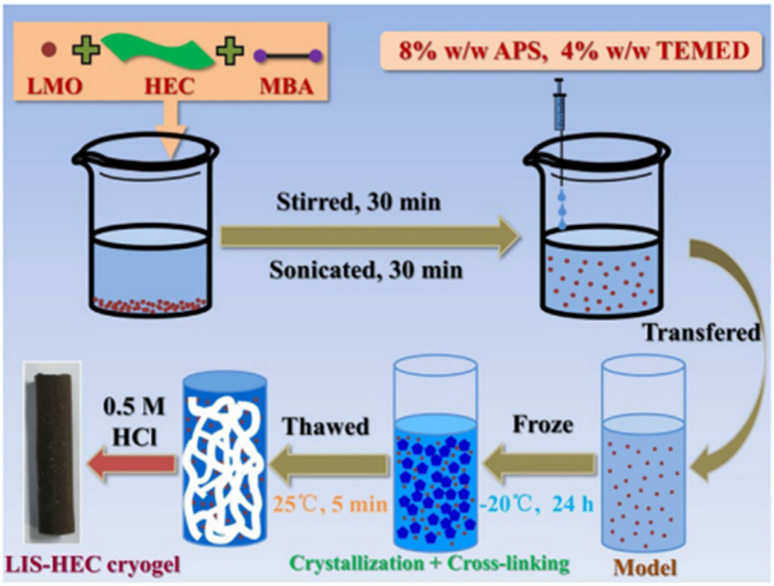

Figure 14. Schematic illustrating of the preparation process for LIS-HEC cryogels. (Reproduced from [73] with permission).

The physicochemical, morphological, thermal, and textural properties of the synthesized cryogels were characterized using XRD, SEM, TGA and BET analysis. Results obtained from batch adsorption studies with LiCl show that alkaline pH condition (pH 9.51) favoured the adsorption of Li ions by the sorbent materials, where the adsorption capacity of LIS powder was 30.5 mg/g. For the LIS-HEC, the results reveal that adsorption capacity increased monotonically with increasing LIS loading up to 80% loading, before it dropped slightly at 100 wt% loading. The authors attributed the drop in adsorption capacity of LIS-HEC-100 to agglomeration of LIS particles on the surface of the cryogel, suggesting a collapse and/or inaccessibility of the templated active binding sites. The adsorption results also revealed that the uptake capacity of LIS-HEC cryogel did not change with increasing loading of LIS but was at an average of 47.8 mg/g. Similarly, results from isotherm studies at pH 9.51 indicate that the adsorption capacity of LIS powder was 44.78 mg/g while LIS-HEC had a higher uptake capacity of 54.23 mg/g. These results show that the cryogel skeleton did not negatively impact on the adsorption properties of LIS particles in the granulated adsorbents. Furthermore, adsorption studies with an artificial brine and seawater shows that the adsorption capacity was 10.64

Preprints.org (www.preprints.org) | NOT PEER-REVIEWED | Posted: 6 February 2024 doi:10.20944/preprints202402.0329.v1

mg/g for brine and 2.46 mg/g for seawater, where the cryogel demonstrated good selectivity for Li ions in both adsorbate systems. Dynamic adsorption studies with the LIS-HEC cryogels revealed that a higher flow rate decreased the time required for attaining adsorption equilibrium, with the consequence of decreased adsorption capacity. The adsorption capacities per unit time of the adsorbents were 22.36, 39.45, 41.67, and 60.39 mg/g/h for flow rates of 1.0, 2.0, 3.0, and 4.0 mL/min, respectively. Reusability studies via multiple adsorption-desorption cycles indicate that the adsorption capacity of the granulated cryogel decreased by 49.11% after nineteen cycles, where the desorption capacity followed the same trend. The decline in adsorption capacity was gradual during the first ten cycles, where the tenth adsorption capacity was 71.25% of the initial value. From the twelfth cycle, the adsorption capacity was stable till a sharp decrease was observed during the twentieth cycle. Similarly, the Mn loss showed the same trend, which indicates that the main reason for the attenuated adsorption capacity was the loss of Mn ions. Reusability results for the LIS-HEC cryogels are presented in Figure 15 where the adsorption-desorption trends show great promise for the HEC cryogel-immobilized Li ion sieves. The synthetic strategy employed by Liu et al. [73] and Xie et al. [54] are similar. Both authors crosslinked the prepared granules, though the crosslinking strategies were different. For example, Liu et al. [73] crosslinked CLS before granulation whereas, Xie et al. [54] crosslinked CLS during and after the granulation process. The results obtained by Xie et al. [54] further affirms the importance of crosslinking before granulation, in agreement with the study by Ding et al. [51].

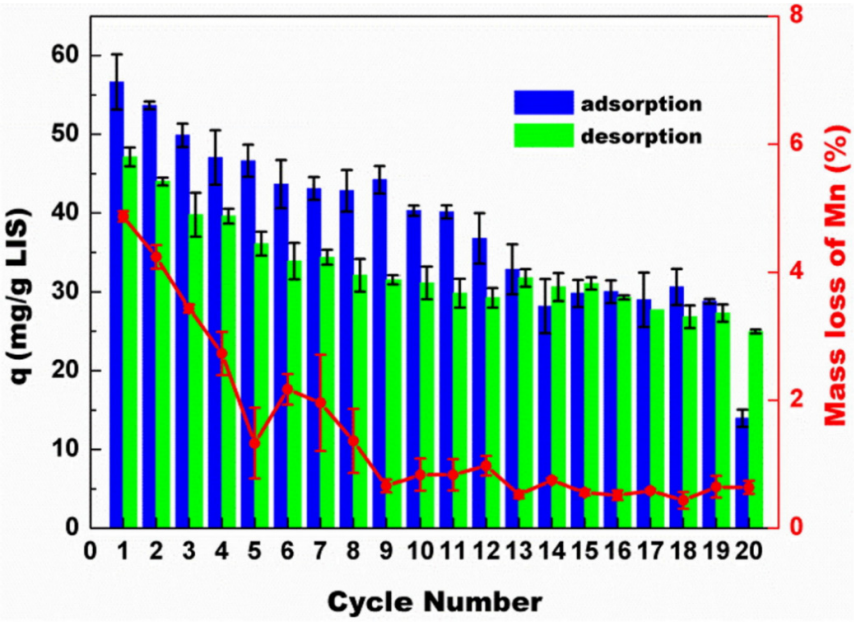

Figure 15. Adsorption-desorption cycling performance of the LIS-HEC-40 cryogel (C0 = 50 mg/L, pH = 9.51). (Reproduced from [73] with permission).

3.2.3. Metal-Based LISs Granulated with Alginate

Alginates (ALGs) are soluble polyanion biopolymers which are biodegradable, non-toxic, and non-irritant in nature. They may be extracted from brown marine algae and bacteria, where α-l-guluronic (G) and β-d-mannuronic (M) are the acid residues (*cf.* Figure 16). ALGs exist commercially mainly in the calcium and sodium salt forms. The species of algae and the G/M ratio along with their distribution along the biopolymer chain influence the properties of ALG that is extracted. Their monosaccharide sequencing and enzymatic controlled reactions make ALGs important biopolymer group for diverse biological and biomedical applications [100–102]. This section of the review highlights the application of ALG as binders for the granulation of Li ion sieves.

Preprints.org (www.preprints.org) | NOT PEER-REVIEWED | Posted: 6 February 2024 doi:10.20944/preprints202402.0329.v1

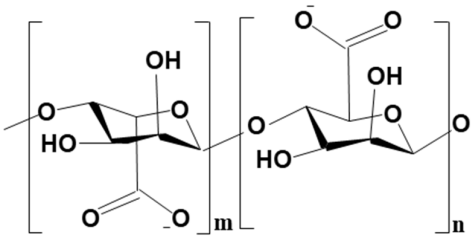

Figure 16. Molecular structure of alginate showing the M and G-blocks.

Luo et al. [24] reported the extraction of Li ions from Salt Lake brines using porous composite LIS mixtures of Li-Al-LDHs (layered double hydroxide) and $NH_4Al_3(SO_4)_2(OH)_6$ crosslinked with sodium ALG as the binding agent. The reaction for the granulation of the composite LISs proceeded as schematically shown in Figure 17. The lithiated LIS precursors were added to a solution of ALG, prepared by dissolving 2.0 g of ALG in 100 mL of deionized water. The resulting mixture was dripped slowly into a 4 wt% $CaCl_2$ solution and held for 24 h for complete crosslinking [103]. The granulated LISs were washed with deionized water till the unreacted chemicals were completely removed.

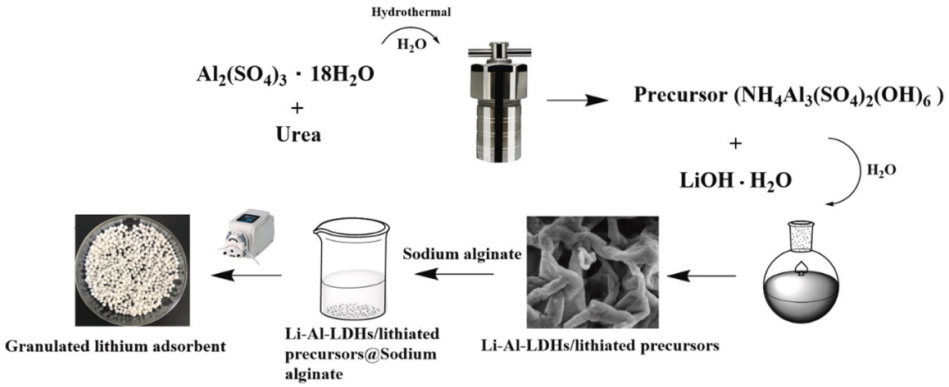

Figure 17. The synthetic route of granulated lithium adsorbents. (Reproduced from [24] with permission).

The precursors and the granulated materials were characterized by FTIR spectroscopy, XRD, XPS spectroscopy, SEM, TEM, thermal analyses, particle size analysis, and BET surface area. Some of the results are presented in Figure 18. The adsorption properties of the granulated LIS were evaluated under the following conditions: adsorbate – LiCl, adsorbate concentration: 500 mg/L, oscillation speed: 200 rpm, temperature: 25 °C, time: 5 – 780 min, and pH: 4 – 10. According to Figure 18a,b, Li uptake by the granulated adsorbents increased initially to a maximum at pH 6 (9.66 mg/g), before it started decreasing. Furthermore, the results show that the concentration and temperature of Li solution had effects on the adsorption capacity of the granulated LISs, whereas the presence of competing ions like NaCl, $MgCl_2$, Na_2SO_4, and KCl in the brines had minor effects on the selectivity of the LISs for Li ions. The adsorption properties of the granulated LIS were further tested with East Taigener Salt Lake brine. Results show that adsorption equilibrium was reached within 180 min, where there was no decline in adsorption capacity (9.16 mg/g) after 5 adsorption-desorption cycles. Mass loss due to dissolution of the granulated LISs was 0.54 % after 10 adsorption-desorption cycles, suggesting that the structural and chemical integrity of the granulated LISs was not compromised after 10 cycles. The structural and chemical resilience was confirmed by FT-IR spectroscopy and XRD analysis as depicted in Figure 18, where the signature peaks of granulated LISs before and after 10 adsorption-desorption cycles are shown.

Preprints.org (www.preprints.org) | NOT PEER-REVIEWED | Posted: 6 February 2024 doi:10.20944/preprints202402.0329.v1

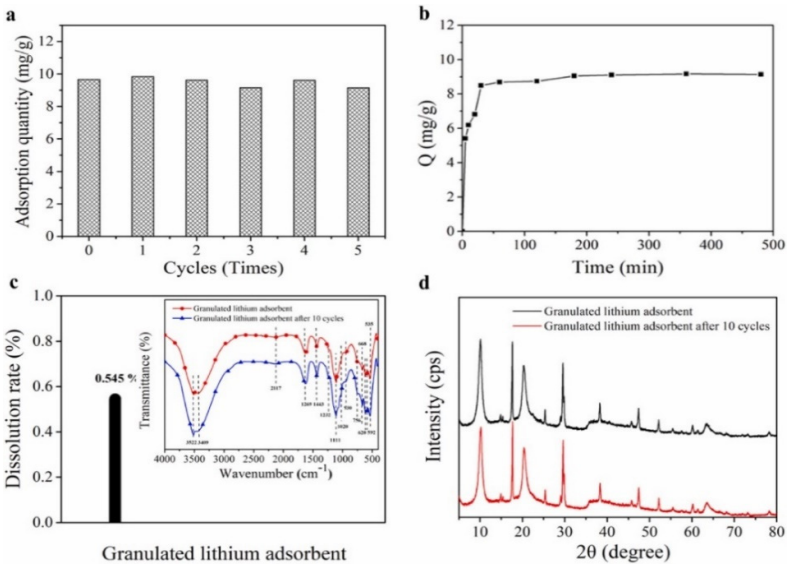

Figure 18. Lithium extraction from East Taigener Salt Lake brine. (a) Adsorption quantity change of granulated adsorbents after 5 adsorption-desorption cycles; (b) Adsorption kinetic curve; (c, d) Dissolution rate of granulated lithium adsorbents, structural change characterized by IR spectroscopy and XRD before and after 10 adsorption-desorption cycles. (Reproduced from [24] with permission).

A similar study by Li et. al. [74] reported the synthesis of granulated Li/Al-LDH adsorbents for the recovery of Li ions from simulated and real Salt Lake brines. The sorbent was prepared by a one-pot dissolution method where LiCl (21.20 g), $AlCl_3 \cdot 6H_2O$ (40.20 g), and urea (100.01 g) were dissolved in 50 mL of deionized water at a 3:1:10 molar ratio and stirred vigorously. Subsequently, 2.12 g of Sodium ALG was dissolved in 200 mL deionized water and mixed with the previous solution at 80 °C for 5 h and heated to 90 °C for 19 h with condensation. The mixture was aged without heating for 12 h, filtered and washed with deionized water, and dried overnight in a vacuum at 45 °C. The dried material was granulated using ALG as the binder in a reaction path as shown in Figure 19, according to the procedure reported by Luo et al. [24].

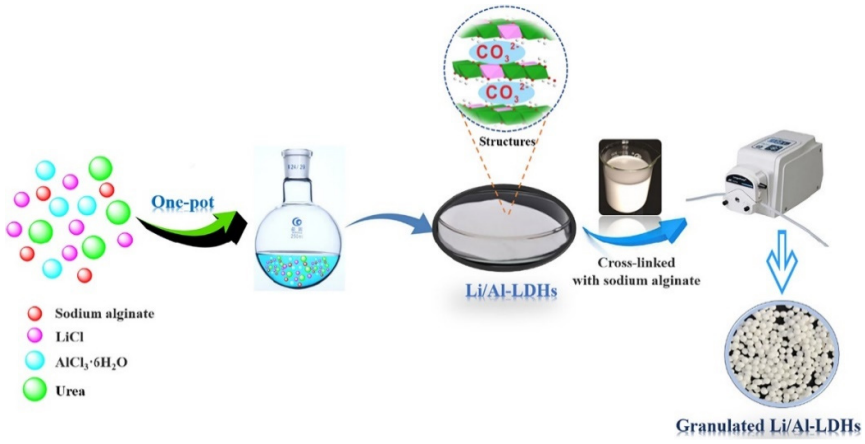

Figure 19. Synthetic route of granulated Li/Al-LDHs. (Reproduced from [74] with permission).

The non-granulated and granulated Li/Al-LDHs Li adsorbents were characterized by FTIR spectroscopy, XRD, SEM, TEM, XPS, and nitrogen adsorption studies. The adsorption properties of the powdered and granulated LISs were evaluated using LiCl as the sorbate, 0.5 g of the adsorbent, concentration range of 20 – 500 mg/L, shaker speed of 200 rpm, pH 4 - 10 and temperature in the range of 25 – 45 °C. The results show that Li adsorption increased with increase in temperature and

Preprints.org (www.preprints.org) | NOT PEER-REVIEWED | Posted: 6 February 2024 doi:10.20944/preprints202402.0329.v1

Li concentration to a maximum of 15.52 mg/g at 45 °C, in agreement with the study reported by Luo et al. [24]. The presence of competing ions had no significant effects on the adsorption properties of the granulated LISs. Reusability studies showed that the granulated LIS maintained 92.2% of the initial adsorption capacity after 6 adsorption-desorption cycles. The adsorption properties of the granulated LISs was further evaluated using East Taigener Salt Lake brine with a Li concentration of 1400 mg/L. The results show that adsorption equilibrium was achieved within 240 minutes, where the adsorption process was best described by the pseudo-second order adsorption kinetic model. The maximum Li adsorption capacity was noted as 14.5 mg/g. The results further affirmed the high selectivity of the granulated LISs for Li ions as evidenced by minimal difference in the concentration of competing ions in the brine before and after the adsorption process. Furthermore, XPS and XRD results before and after 10 adsorption-desorption cycles supported the mechanical and chemical stability of the granulated LIS sorbents (data/results not shown). The chemical and mechanical stability of the granules prepared by Luo et al. [24] and Li et. al. [74] are very similar as expected, because of the very similar synthetic strategies employed by the authors, where crosslinking was performed before granulation. In particular, the granules prepared by both authors were from Al-based precursors and displayed little or no attenuation of adsorption properties after 10 adsorption-desorption cycles. The results of these studies further affirm the role of crosslinking before granulation on the chemical and mechanical stability of the granulated adsorbents as previously highlighted by the studies of Xie et al. [54] and Ding et al. [51].

Koilraj et al. [75] reported the encapsulation of powdery spinel-type LISs derived from biogenic manganese oxide (LMO) in ALG beads. The biogenic LISs were granulated using ALG as the binder as follows: Following acid treatment of the biogenic LMO for 12 h to obtain the biogenic HMO, approximately 0.4 g of the HMO was suspended in 20 mL of water and continuously stirred for 1 h. 0.35 g of sodium ALG (1.5 w/v%) was then added to the mixture at 60 °C under vigorous stirring for 1 h to obtain a homogenous LMO-sodium ALG suspension. Bead formation was achieved by slow dropping of the suspension into 200 mL 0.2 M $CaCl_2$ solution using a disposable syringe with an inner diameter of 0.8 mm. The resulting beads were aged for 12 h, washed 3 times with decarbonized water to remove unreacted chemicals, and stored in water prior to use. Blank alginate (ALG) beads without the HMO LISs were also prepared. Characterization of the powdery and granulated adsorbent materials was achieved by XRD, SEM and TEM studies. Batch adsorption studies with a solution containing 4.23 mM Li ions and the granulated biogenic HMO-ALG LIS, powdery HMO and ALG bead at a solid to liquid ratio of 1.0 g/L were performed and results are shown in Figure 20. The results show that HMO powder had a maximum adsorption capacity of 3.67 mmol/g, 0.17 mmol/g for ALG beads and 3.59 mmol/g for granulated HMO-ALG LIS, corresponding to 2.06 mmol/g based on a dry weight of HMO-ALG beads. The results show that adsorption of Li ions by HMO–ALG LISs mainly occurs in the HMO domain of the granulated LIS whereas encapsulation of HMO in the sodium ALG matrix did not negatively impact the adsorption properties of HMO LIS. The change in adsorption properties of the granulated LIS due to multiple usage was evaluated and the results reveal that there was a slight decline in the adsorption capacity with an increase in the number of adsorption-desorption cycles (*cf.* Figure 20). The authors attributed the slight decline to Mn loss through dissolution due to acid treatment during desorption. Furthermore, the granulated LISs maintained more than 90% of its adsorption capacity in the 5th cycle, consistent with the results of a non-granulated LISs reported in a previous study [104]. The synthetic strategy reported by Koilraj et al. [75] is slightly different than that of Luo et al. [24] and Li et. al. [74], where the later authors used Al-based LIS precursors relative to Mn-based precursor by Koilraj et al. [75].

Preprints.org (www.preprints.org) | NOT PEER-REVIEWED | Posted: 6 February 2024 doi:10.20944/preprints202402.0329.v1

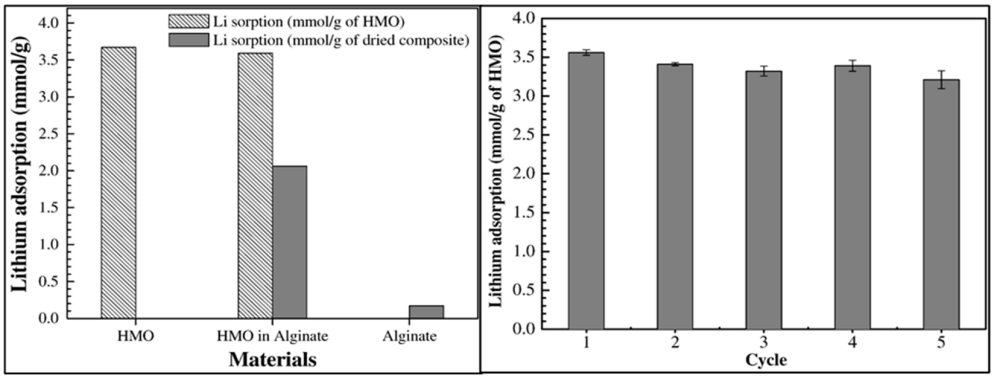

Figure 20. Comparison of the adsorption capacity of Li+ to different materials. Initial Li+ concentration 4.23 mM, volume 20 mL, mass of HMO 20 mg, mass of wet HMO–Al beads 0.56 g (corresponding to 20 mg HMO), pH 8.5, and time 24 h. Change in the Li+ adsorption capacity to HMO-AL beads with reuse time. For adsorption: Initial Li+ concentration 4.23 mM in 0.1 M CaCl2, volume 20 mL, mass of wet HMO–Al beads 0.56 g (corresponding to 20 mg HMO), pH 8.5, and time 24 h. For desorption: 40 mL mixture of 0.1 M HCl and 0.1 M CaCl2 for 12 h. (Reproduced from [75] with permission).

In another study, a novel strategy was employed to separate Li ions from concentrated seawater using a synergistic effect of Al^{3+}- crosslinked ALG and hydrogen manganese oxide (HMO) [76]. The crosslinked Al^{3+} in the ALG network structure generates a strong repulsive force to isolate salt cations from competition with Li ions for adsorptive binding sites in the adsorbate composites. Preparation of the LIS-ALG composites was done follows: 0.5 g of LIS (LMO) was added to 400 mL of 2.5 wt% aqueous ALG solution. The mixture was vigorously mixed with the aid of a sonicator. Granulation was carried out by dropping the mixture into a 5 wt% $AlCl_3$ solution using a peristaltic pump. The prepared granulated LIS was washed with deionized water until the conductivity of the wastewater was similar to that of deionized water. The granulated LIS was dried in a humidity oven operating at room temperature and relative humidity in the range of 65-70%. Delithiation was carried out by treatment of 0.4 g of the granulated LIS with 400 mL of 1.0 M HCl. Following delithiation, the granulated HMO/AlG(Al) LIS was washed with deionized water and dried at room temperature. Another sample (HMO/AlG(Zr) was prepared through the same procedure, except changing the crosslinking agent to $ZrCl_4$. A control sample, AlG(Al) was prepared according to the same procedure but without the addition of LMO. The structural and morphological properties of the synthesized materials were elucidated through XRD, TEM and SEM studies.

The effect of competing ions on the adsorption properties of HMO/AlG(Al) was evaluated by measuring the concentrations of Li^+, Na^+, K^+, and Mg^{2+} in a multi-ion solution matrix where the initial concentration of each ion was 750 mg L^{-1}. The results show that the adsorption capacities for Li ions at 0.5, 1, and 3 h were 0.223, 0.263, and 0.363 mmol/g, respectively, where the adsorption capacity increased more than 1.6 times at the end of a 3 h incubation period. On the other hand, the adsorption capacities for Na^+, K^+, and Mg^{2+} increased 1.1, 1.8 and 1.4 times for various incubation times (30 – 180 min) (*cf.* Figure 21). The results suggest that the granulated HMO/AlG(Al) can selectively adsorb Li ions in the presence of other cations, though with a lower affinity for Li ions, relative to other recently developed Li ion sieves [105]. The choice of various LIS granulation techniques suggests that numerous LIS materials with diverse properties and applications may be synthesized.

Preprints.org (www.preprints.org) | NOT PEER-REVIEWED | Posted: 6 February 2024 doi:10.20944/preprints202402.0329.v1

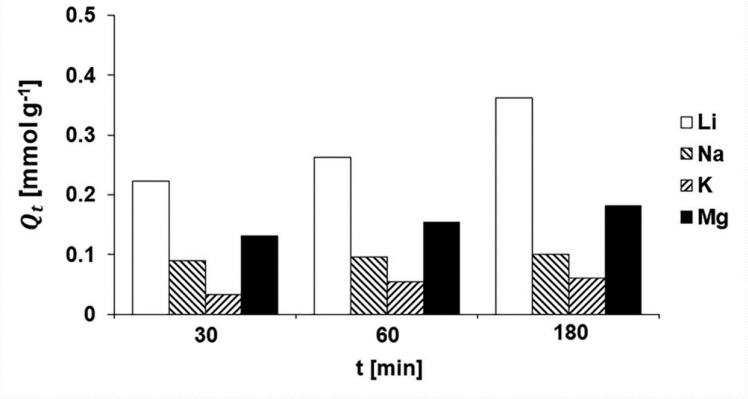

Figure 21. Comparisons of adsorption capacities of HMO/Alg(Al) for Li+, Na+, K+, and Mg2+ cations from multi-ion solutions containing 750 mg L−1 of each salt cation according to incubation time. (Reproduced from [76] with permission).

The adsorption property of the granulated HMO/AlG(Al) sieve was also evaluated using concentrated seawater with a Li concentration of 4 mg/L and more than 100 g/L of competing ions. The results show that the granulated HMO/AlG(Al) LIS display a high affinity for Li ions with the selectivity separation factors of 36.36 of α_{Na}^{Li}, and 40.08 of α_{K}^{Li} for Na and Li, along with a negligible adsorption capacity for Mg ions respectively. This result demonstrates high selectivity for Li ions from a complex matrix. However, during the second cycle, the Li ion selectivity largely decreased because a large amount of Na^+, K^+, and Mg^{2+} ions were captured. The authors attributed the drop in selectivity of the granulated LIS to a compromise on structural integrity due to extensive swelling that may result in the extraction of HMO particles from the matrix. The authors also evaluated the adsorption properties of another granulated LIS, crosslinked with $ZrCl_4$. The results show that the adsorption capacity for Li ions increased while the competing ions were rejected, where the selectivity separation factors of Li vs Na (α_{Na}^{Li}) and Li vs K(α_{K}^{Li}) for HMO/AlG(Zr) increased from 3.71 and 5.78 at the first cycle to 36.9 and 70.0 at the third cycle, respectively. The authors claimed that the increased selectivity for Li ions by HMO/AlG(Zr) may be attributed to the reorganization of Zr^{4+}–AlG network or to the continued delithiation through repetitive acid exposure, which is completely different from the behaviour of HMO/AlG(Al). In addition, the Zr^{4+}–crosslinked ALG network structure enhances structural stability and reusability due to ionic crosslinking between Zr^{4+} ions and two, three or even four carboxyl groups of ALG [55]. Thus, this structural coordination with many carboxyl groups induces very low swelling compared with the Al^{3+}–crosslinked ALG composites. The results reported by Park et al. [76] further highlights the role of crosslinkers on the chemical and mechanical stability as well as selectivity for Li ions by granulated adsorbents.

3.2.4. Metal-Based LISs Granulated with Agar

Agar (AG) is a biopolymer that belongs to the polysaccharide family and is extracted from specific species of marine red algae from the Rhodophyceae class [106,107]. The two main commercial sources of this biopolymer are *Gelidium* sp. and *Gracilaria* sp. AG forms a supporting structure in the cellular walls of the seaweeds [106,108,109]. Its chemical structure consists of a mixture of agaropectin (non-gelling fraction) and agarose (gelling fraction) [108,110]. Agarose is a linear polysaccharide consisting of repetitive units of D-galactose and 3-6-anhydro-L-galactose, linked by alternating α-(1 → 3) and β-(1 → 4) glycosidic bonds (*cf.* Figure 22). On the other hand, agaropectin is slightly branched and sulphated. Interest in the use of AG as a binder for the granulation of LISs relates to its gel forming properties in hot water, where the gel forming ability is a result of its ability to form hydrogen bonds between agarose molecules [106,108,111]. This section of the review will highlight recent progress in the application of AG as binders for the granulation of metal based LISs.

Preprints.org (www.preprints.org) | NOT PEER-REVIEWED | Posted: 6 February 2024 doi:10.20944/preprints202402.0329.v1

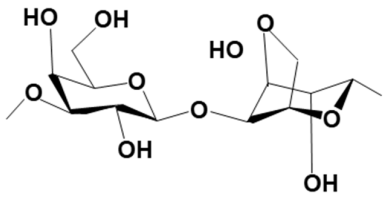

Figure 22. Molecular structure of Agar.

Various studies have reported on the granulation of LISs using AG as the binding agent. For example, Han et. al. [78] have prepared AG-based mm-sized spherical ion-sieve foams (SIFs) with hierarchical pore structure from LMO for the recovery of Li ions from seawater. The granulated LISs were prepared via a mechanical foaming method, drip-in-oil and AG gelation processes [112]. According to the authors, a 60 wt.% slurry of LMO was prepared using deionized water and the temperature of the slurry maintained at 60 °C. Foaming was achieved via the addition of 4 mL/L of sodium lauryl sulphate to the slurry, followed by the addition of AG solution of different concentrations (2, 3, 4 or 6%). The slurry was granulated by dripping into liquid paraffin solution (height = 50 cm and temperature = 5 °C) at a flow rate of 10 cm^3 min^{-1} using a syringe with an inner diameter of 2.4 mm. During foaming and dripping, the slurry temperature was maintained at 60 °C. The resulting granulated and gelled LIS spheres were collected from the bottom of the liquid paraffin column, dried at room temperature for a week, and then washed in water/ethanol at 5 °C for 1 h to remove any oil and surfactant from the samples. Delithiation was achieved by treating the granules with 0.5 M HCl at 25 °C for 5 days, followed by drying at room temperature for 24 h. The LMO obtained after acid treatment were designated as HMO, while the granules were designated as (SIFs)-*x*, respectively, where *x* indicates the mass percentage of AG in the granules. The starting materials and the granules were characterized via XRD, FE-SEM, mercury porosimetry, pycnometry, and nitrogen adsorption-desorption studies.

Evaluation of the adsorption properties of the LMO, HMO and the SIFs were performed using 0.1 M LiOH at pH 13. The results of adsorption studies with LiOH show that uptake capacity was negligible for LMO, 24.1 mg/g for HMO, 20.9 mg/g for SIFs-2 and 2.7 mg/g for SIFs-6. The results indicate that the adsorption capacity of HMO was greater than that of SIFs-2, which exhibited the best adsorption capacity among the SIFs with different AG contents. Due to the hierarchical pore structure and highest uptake capacity, SIFs-2 granules and HMO were used for the adsorption experiments with seawater with a Li concentration of 0.17 mg/L at pH 8. The results reveal that HMO and SIFs-2 had adsorption capacities of 16.7 mg/g and 3.4 mg/g respectively. Furthermore, the reusability of SIFs-2 granules was tested with seawater, where the results indicate a minor loss (4.2%) in adsorption capacity, while the desorption efficiency was maintained at approximately 86%, over 5 adsorption-desorption cycles as shown in Figure 23.

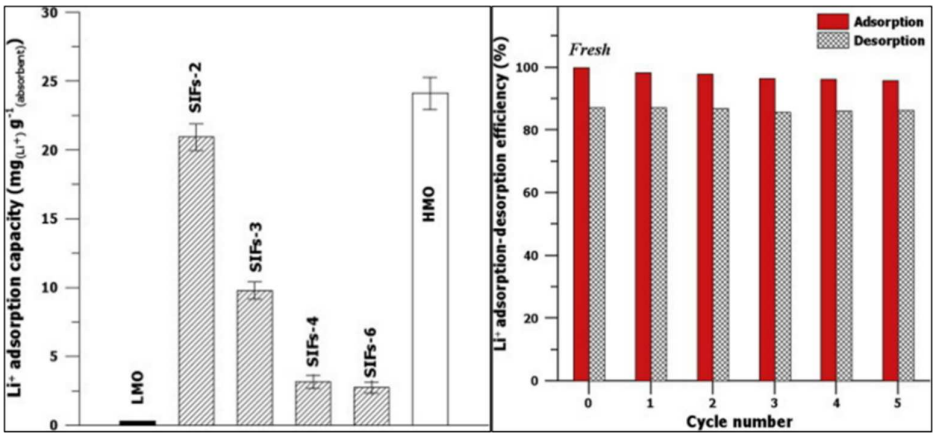

Preprints.org (www.preprints.org) | NOT PEER-REVIEWED | Posted: 6 February 2024 doi:10.20944/preprints202402.0329.v1

Figure 23. Lithium adsorption capacities for LMO, HMO, and SIFs with different agar contents. The tests for Li^+ adsorption capacity were carried out in 0.1 M LiOH (pH 13) for 24 h at 25 °C. Li^+ adsorption–desorption efficiency of SIFs-2 in natural seawater as a function of the cycle number. The red and grid bars represent the adsorption and desorption efficiencies, respectively. (Reproduced from [78] with permission).

The adsorption properties of Ti-based LISs identified as ion sieves (ISs) and porous ions sieves (PISs) with enhanced post-separation ability and high-performance Li recovery from geothermal water was reported by Chen et al. [79]. The reaction process for the ISs and PISs are schematically shown in Figure 24 and described as follows: Li_2TiO_3 (LTO) precursor was delithiated using 0.25 M HCl at a mass/volume ratio of 1 g/L at 333 K for 12 h to obtain the corresponding HTO powder. Following delithiation, the HTO powder and AG were mixed at variable mass ratios (1:1, 2:1, 3:1, 4:1 and 5:1) using deionized water and heated to 373 K with stirring until the AG became molten. The resulting molten slurry was granulated by dropping into cold simethicone via an injector. The granules were left in the granulation solution for 24 h, cleaned using petroleum ether and dried to obtain the granulated LIS (IS-1 to IS-5). The corresponding PIS were obtained after calcination of IS in air at 823 K for 1 h (*cf.* Figure 24).

Figure 24. Schematic diagram of the synthesis of titanium-based ions sieves (Iss) and and porous ion sieves (PISs). (Reproduced from [79] with permission).

Structural and morphological properties of the granulated LISs were elucidated via XRD, TGA, TG-DSC, SEM, TEM, nitrogen adsorption and XPS studies. Adsorption properties of the granulated LISs (ISs and PISs) was evaluated at pH 12 and 333 K. The Li adsorption capacity of IS and PIS increased with increasing concentration of HTO and achieved a maximum at HTO: AG ratio of 4:1 in both IS and PIS, where the adsorption performance of PIS was better than that of IS because of its mesoporous structure. Due to the superior adsorption capacity of PIS-4, it was used for further studies. Further experiments revealed that the adsorption process was favoured by alkaline pH conditions, uptake increased with increasing temperature and Li ion concentration in solution, and adsorption equilibrium was achieved in 4 h. Based on the Langmuir adsorption model, the maximum adsorption capacity of PSI-4 was 34.23 mg/g. The granulated LISs (PIS-4) were further evaluated for its ability to recover Li ions from geothermal water containing competitive ions (Na^+, K^+ and Ca^{2+}), where the initial concentrations of Li^+, Na^+, K^+ and Ca^{2+} in the geothermal water were 25.8, 682.1, 137.9 and 211.1 mg/L, respectively at pH 8.80. The pH of the geothermal water was adjusted to 12 using NaOH solution. The Li removal efficiency of PIS-4 was 95.3%, while the separation factors for competing ions were 1162.3, 273.7 and 328.5 for Na^+, K^+ and Ca^{2+}, respectively, in agreement with the ion sieving effect of PIS-4. To further evaluate the effects of competing ions like Mg^{2+}, a binary solution containing Li and Mg ions was prepared, where the concentration of Li^+ and Mg^{2+}in solution was fixed at 25 mg/L and 50, 100 and 200 mg/L respectively. The results obtained show that increasing the concentration of Mg^{2+} in solution had negligible effects on the adsorption capacity of PIS-4. Reusability of the granulated PIS-4 was evaluated using variable concentrations of HCl solution. The results show that the desorption efficiency of Li ions gradually increased with increasing HCl concentration till 0.25 mol/L, where the increase was negligible, but the dissolution of Ti increased

Preprints.org (www.preprints.org) | NOT PEER-REVIEWED | Posted: 6 February 2024 doi:10.20944/preprints202402.0329.v1

significantly. Furthermore, it was noted that PIS-4 was more chemically stable than HTO which had a 4.2% mass loss due to Ti dissolution in 0.5 M HCl relative to 1.2% by the earlier. Due to Ti dissolution at high HCl concentrations, 0.25 M HCl was chosen as the desorption solution. The authors reported that the adsorption and desorption efficiencies of PIS-4 did not display a significant change after 12 adsorption-desorption cycles as evidenced in Figure 25.

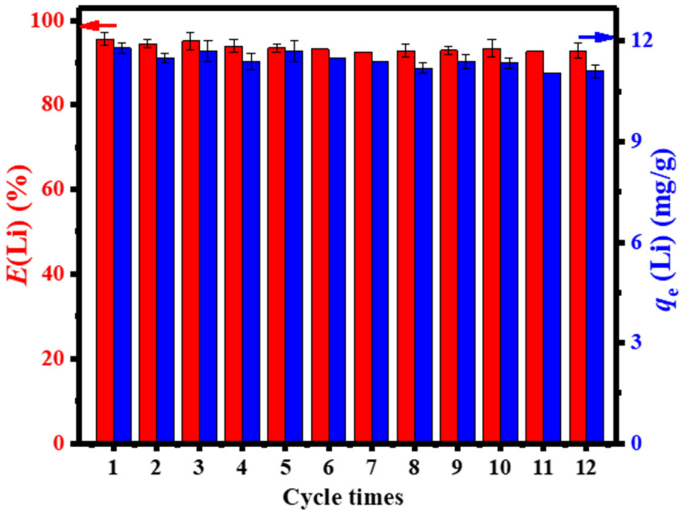

Figure 25. The reusability of PIS-4 with 12-times adsorption-desorption cycles. (Reproduced from [79] with permission).

4. Comparison of the Sorption Properties of Granulated LISs

In this section, we report the adsorption properties of various granulated LISs to compare the efficiency of the different types of binding and crosslinker agents. Table 1 summarizes the uptake capacities for a variety of granulated LISs that were prepared from various biopolymer and crosslinker agents and evaluated in different brine adsorbate solutions. The crosslinker molecules used include sulfuric acid, ECH, EDGE, and GLY, while spiked seawater, concentrated seawater, geothermal water and LiCl were used as adsorbates. The results show that the LISs granulated with CTS as the binder displayed adsorption capacities in the range of 5 to 54.7 mg/g, where the highest adsorption capacity was displayed by the granules crosslinked with sulfuric acid. The CTS-based granules crosslinked with ECH exhibited the most efficient adsorption-desorption performance at 6 cycles, where the performance may be related to the two-step cross-linking strategy. On the other hand, the LISs granulated with various forms of CLS revealed uptake capacities in the range of 12 to 54.2 mg/g with the highest adsorption capacity and reusability (20 adsorption-desorption cycles) displayed by the granule crosslinked with N, N′-methylenebis (acrylamide) (MBA). In the case of ALG based granulated LISs, the adsorption capacity was in the range of 2.52 to 24.9 mg/g, where $CaCl_2$ was the most common crosslinker used for the granulation process. As for the AG based granulated LISs, the adsorption capacities were estimated between 3.40 to 12.3 mg/g respectively. One of the challenges faced in the direct comparison of adsorption capacities is the use of variable adsorption conditions such as adsorbate concentration and type, pH, as well as the solid to liquid ratio during the studies. This challenge limits the direct comparison of the granulated adsorbents and identification of the most suitable binder for the LISs presented in this review.

Table 1. Uptake Capacities of Granulated LIS.

S/N	Binder	Crosslinker	Sorbate	Uptake capacity (mg/g)	Reference
1	Chitosan	Sulfuric acid	Spiked seawater	10.0	Hong et al. [49]
2	Chitosan	Sulfuric acid	Spiked seawater	54.7	Ryu et al. [50]

Preprints.org (www.preprints.org) | NOT PEER-REVIEWED | Posted: 6 February 2024 doi:10.20944/preprints202402.0329.v1

3	Chitosan	ECH and EDGE	Geothermal water	11.4	Ding et al. [51]
4	Chitosan	ECH	LiCl	5.0	Yüksel Özşen and Kahvecioğlu [52]
5	Chitosan	EDGE, ECH and glutaraldehyde	Geothermal water	8.98	Wang et al. [53]
6	Cellulose	NA	LiCl	28.6	Qian et al. [71]
7	Carboxymethyl cellulose	$FeCl_3$, EDGE and ME	Geothermal water	12.0	Xie et al. [54]
8	Bacterial cellulose	NA	LiCl	35.5	Zhang et al. [72]
9	Hydroxyethyl cellulose	MBA	LiCl	54.2	Liu et al. [73]
10	Sodium alginate	$CaCl_2$	Salt Lake brine	9.16	Luo et al. [24]
11	Sodium alginate	$CaCl_2$	Salt Lake brine	14.5	Li et al. [74]
12	Sodium alginate	$CaCl_2$	LiCl	24.9	Koilraj et al. [75]
13	Sodium alginate	$AlCl_3$/ $ZrCl_4$	Concentrated seawater	2.52	Park et al. [76]
14	Agar	NA	Seawater	3.40	Han et al. [78]
15	Agar	NA	Geothermal water	12.3	Chen et al. [79]

5. Conclusions

This study has highlighted recent progress in the use of various biopolymers, namely chitosan (CTS), cellulose (CLS), alginate (ALG) and agar (AG), as binders for the granulation of lithium-ion sieves (LISs). Granulation is the most viable method for producing mechanically stable LIS microspheres with improved adsorption-desorption performance from micro/nano-based powdered sieves. Various granulation processes have been reported for lithium manganese oxide (LMO)- and lithium titanium oxide (LTO)-based sieves employing CTS, CLS, ALG, and AG as the binding agents to achieve materials with improved adsorption and mechanical properties. Generally, biopolymers have diverse functional groups (e.g., OH, NH, and C=O) that can be involved in H-bonding and crosslinking reactions to form 3D structures with a multitude of active binding sites for Li templation. The structural and performance properties of the biopolymer-granulated LISs were characterized using spectroscopic (e.g., FTIR), imaging (SEM), X-ray diffraction, batch adsorption studies, and adsorption-desorption tests using acids as eluents. While variable adsorbates (e.g., brine, LiCl, LiOH and seawater etc.) and adsorption conditions (e.g., temperature, pH and solid to liquid ratio etc.) were used for the studies, it is concluded that the modification of the adsorption performance for the various biopolymer-granulated LISs varies in accordance with the following factors: 1) the presence of abundant active binding sites in the LISs structure, 2) the surface and textural properties of the LISs material, and 3) the nature of the adsorbate matrix. Similarly, the recyclability (adsorption-desorption) performance is accounted for by; 1) the nature of the coordination interactions between the Li ion and the adsorption site, 2) the structural integrity/morphology of the LISs granules, and 3) the mechanical/chemical stability of the 3D structure of the granulated LISs. The mechanical/chemical stability of the LISs can be further enhanced through crosslinking of the sieves pre- and/or post-granulation. Several crosslinker agents, such as sulphate anions, GLY, EDGE, $CaCl_2$, $FeCl_3$, $AlCl_3$ and $ZrCl_4$, have been employed in this study with various performance outcomes. The choice of the crosslinker is essential to the desired LISs properties, in terms of the adsorption-desorption performance and their selectivity for Li ions in a matrix containing competing ions (e.g., Na, K, Mg, and Ca). However, it is generally concluded from this review study that crosslinking prior to granulation leads to LISs materials with greater stability. In particular, a multi-step crosslinking strategy employed prior to, and post-granulation can afford LIS materials with overall better adsorption properties and structural integrity due to the introduction of multiple active binding sites for Li ions, along with improved stability of the heavily crosslinked granules. Finally, the review reveals that there are no studies on the use of CTS as a binder for the granulation of LTO and Li/Al-LDH based LIS materials, use of ALG for the granulation of LTO based LIS as well as the use of AG for Li/Al-LDH based LIS materials. This therefore calls for more studies on the use of these abundant

Preprints.org (www.preprints.org) | NOT PEER-REVIEWED | Posted: 6 February 2024 doi:10.20944/preprints202402.0329.v1

and environmentally friendly biomaterials as binders for the granulation of metal-based Li ion sieves to unlock its potential for the Li mining industry.

Acknowledgments/Funding: This research did not receive any specific grant from funding agencies in the public, commercial, or not-for-profit sectors.

References

1. Haddad AZ, Hackl L, Akuzum B, Pohlman G, Magnan J-F, Kostecki R. How to make lithium extraction cleaner, faster and cheaper - in six steps. Nature 2023;616:245–8. https://doi.org/10.1038/d41586-023-00978-2.
2. Jaskula BW. Mineral Commodity Summaries. LITHIUM. US Geological Survey, Mineral Commodity Summaries, January 2021. https://pubs.usgs.gov/periodicals/mcs2021/mcs2021-lithium.pdf (accessed May 24, 2023).
3. Weng D, Duan H, Hou Y, Huo J, Chen L, Zhang F, et al. Introduction of manganese based lithium-ion Sieve-A review. Progress in Natural Science: Materials International 2020;30:139–52.
4. Ambrose H, Kendall A. Understanding the future of lithium: Part 1, resource model. J Ind Ecol 2020;24:80–9. https://doi.org/https://doi.org/10.1111/jiec.12949.
5. Battistel A, Palagonia MS, Brogioli D, La Mantia F, Trócoli R. Electrochemical Methods for Lithium Recovery: A Comprehensive and Critical Review. Advanced Materials 2020;32:1905440. https://doi.org/https://doi.org/10.1002/adma.201905440.
6. Yu H, Naidu G, Zhang C, Wang C, Razmjou A, Han DS, et al. Metal-based adsorbents for lithium recovery from aqueous resources. Desalination 2022;539:115951. https://doi.org/https://doi.org/10.1016/j.desal.2022.115951.
7. Zhang Y, Hu Y, Wang L, Sun W. Systematic review of lithium extraction from salt-lake brines via precipitation approaches. Miner Eng 2019;139:105868. https://doi.org/https://doi.org/10.1016/j.mineng.2019.105868.
8. Wang H, Zhong Y, Du B, Zhao Y, Wang M. Recovery of both magnesium and lithium from high Mg/Li ratio brines using a novel process. Hydrometallurgy 2018;175:102–8. https://doi.org/https://doi.org/10.1016/j.hydromet.2017.10.017.
9. Shi D, Cui B, Li L, Xu M, Zhang Y, Peng X, et al. Removal of calcium and magnesium from lithium concentrated solution by solvent extraction method using D2EHPA. Desalination 2020;479:114306. https://doi.org/https://doi.org/10.1016/j.desal.2019.114306.
10. Jiang H, Zhang S, Yang Y, Yu J. Synergic and competitive adsorption of Li–Na–MgCl2 onto lithium–aluminum hydroxides. Adsorption 2020;26:1039–49. https://doi.org/10.1007/s10450-020-00208-5.
11. Wang J, Yue X, Wang P, Yu T, Du X, Hao X, et al. Electrochemical technologies for lithium recovery from liquid resources: A review. Renewable and Sustainable Energy Reviews 2022;154:111813. https://doi.org/https://doi.org/10.1016/j.rser.2021.111813.
12. Quist-Jensen CA, Ali A, Drioli E, Macedonio F. Perspectives on mining from sea and other alternative strategies for minerals and water recovery – The development of novel membrane operations. J Taiwan Inst Chem Eng 2019;94:129–34. https://doi.org/https://doi.org/10.1016/j.jtice.2018.02.002.
13. Ryu T, Lee D-H, Ryu JC, Shin J, Chung K-S, Kim YH. Lithium recovery system using electrostatic field assistance. Hydrometallurgy 2015;151:78–83. https://doi.org/https://doi.org/10.1016/j.hydromet.2014.11.005.
14. Li X, Mo Y, Qing W, Shao S, Tang CY, Li J. Membrane-based technologies for lithium recovery from water lithium resources: A review. J Memb Sci 2019;591:117317. https://doi.org/https://doi.org/10.1016/j.memsci.2019.117317.
15. Paredes C, Rodríguez de San Miguel E. Selective lithium extraction and concentration from diluted alkaline aqueous media by a polymer inclusion membrane and application to seawater. Desalination 2020;487:114500. https://doi.org/https://doi.org/10.1016/j.desal.2020.114500.
16. Sun Y, Wang Q, Wang Y, Yun R, Xiang X. Recent advances in magnesium/lithium separation and lithium extraction technologies from salt lake brine. Sep Purif Technol 2021;256:117807. https://doi.org/https://doi.org/10.1016/j.seppur.2020.117807.
17. Zhang J, Cheng Z, Qin X, Gao X, Wang M, Xiang X. Recent advances in lithium extraction from salt lake brine using coupled and tandem technologies. Desalination 2023;547:116225. https://doi.org/https://doi.org/10.1016/j.desal.2022.116225.
18. Hu S, Sun Y, Pu M, Yun R, Xiang X. Determination of boundary conditions for highly efficient separation of magnesium and lithium from salt lake brine by reaction-coupled separation technology. Sep Purif Technol 2019;229:115813. https://doi.org/https://doi.org/10.1016/j.seppur.2019.115813.
19. Swain B. Recovery and recycling of lithium: A review. Sep Purif Technol 2017;172:388–403. https://doi.org/https://doi.org/10.1016/j.seppur.2016.08.031.

Preprints.org (www.preprints.org) | NOT PEER-REVIEWED | Posted: 6 February 2024 doi:10.20944/preprints202402.0329.v1

20. Hamzaoui AH, M'nif A, Hammi H, Rokbani R. Contribution to the lithium recovery from brine. Desalination 2003;158:221–4. https://doi.org/https://doi.org/10.1016/S0011-9164(03)00455-7.
21. Masmoudi A, Zante G, Trébouet D, Barillon R, Boltoeva M. Solvent extraction of lithium ions using benzoyltrifluoroacetone in new solvents. Sep Purif Technol 2021;255:117653. https://doi.org/https://doi.org/10.1016/j.seppur.2020.117653.
22. Liu G, Zhao Z, Ghahreman A. Novel approaches for lithium extraction from salt-lake brines: A review. Hydrometallurgy 2019;187:81–100. https://doi.org/https://doi.org/10.1016/j.hydromet.2019.05.005.
23. Hong H-J, Ryu T, Park I-S, Kim M, Shin J, Kim B-G, et al. Highly porous and surface-expanded spinel hydrogen manganese oxide (HMO)/Al2O3 composite for effective lithium (Li) recovery from seawater. Chemical Engineering Journal 2018;337:455–61. https://doi.org/https://doi.org/10.1016/j.cej.2017.12.130.
24. Luo Q, Dong M, Nie G, Liu Z, Wu Z, Li J. Extraction of lithium from salt lake brines by granulated adsorbents. Colloids Surf A Physicochem Eng Asp 2021;628:127256. https://doi.org/https://doi.org/10.1016/j.colsurfa.2021.127256.
25. Safari S, Lottermoser BG, Alessi DS. Metal oxide sorbents for the sustainable recovery of lithium from unconventional resources. Appl Mater Today 2020;19:100638. https://doi.org/https://doi.org/10.1016/j.apmt.2020.100638.
26. Orooji Y, Nezafat Z, Nasrollahzadeh M, Shafiei N, Afsari M, Pakzad K, et al. Recent advances in nanomaterial development for lithium ion-sieving technologies. Desalination 2022;529:115624. https://doi.org/https://doi.org/10.1016/j.desal.2022.115624.
27. Torrejos REC, Nisola GM, Song HS, Limjuco LA, Lawagon CP, Parohinog KJ, et al. Design of lithium selective crown ethers: Synthesis, extraction and theoretical binding studies. Chemical Engineering Journal 2017;326:921–33. https://doi.org/https://doi.org/10.1016/j.cej.2017.06.005.
28. Oral I, Tamm S, Herrmann C, Abetz V. Lithium selectivity of crown ethers: The effect of heteroatoms and cavity size. Sep Purif Technol 2022;294:121142. https://doi.org/https://doi.org/10.1016/j.seppur.2022.121142.
29. Dong M, Luo Q, Li J, Wu Z, Liu Z. Lithium adsorption properties of porous LiAl-layered double hydroxides synthesized using surfactants. Journal of Saudi Chemical Society 2022;26:101535. https://doi.org/https://doi.org/10.1016/j.jscs.2022.101535.
30. Suresh P, Sreedhar I, Vaidhiswaran R, Venugopal A. A comprehensive review on process and engineering aspects of pharmaceutical wet granulation. Chemical Engineering Journal 2017;328:785–815. https://doi.org/https://doi.org/10.1016/j.cej.2017.07.091.
31. Ooi K, Miyai Y, Katoh S, Maeda H, Abe M. Topotactic lithium (1+) insertion to. lambda.-manganese dioxide in the aqueous phase. Langmuir 1989;5:150–7.
32. Kozawa A, Powers RA. The Manganese Dioxide Electrode in Alkaline Electrolyte; The Electron-Proton Mechanism for the Discharge Process from MnO2 to MnO1.5. J Electrochem Soc 1966;113:870. https://doi.org/10.1149/1.2424145.
33. Hunter JC. Preparation of a new crystal form of manganese dioxide: λ-MnO2. J Solid State Chem 1981;39:142–7.
34. Yang X, Kanoh H, Tang W, Ooi K. Synthesis of Li1. 33Mn1. 67O4 spinels with different morphologies and their ion adsorptivities after delithiation. J Mater Chem 2000;10:1903–9.
35. Chitrakar R, Sakane K, Umeno A, Kasaishi S, Takagi N, Ooi K. Synthesis of orthorhombic LiMnO2 by solid-phase reaction under steam atmosphere and a study of its heat and acid-treated phases. J Solid State Chem 2002;169:66–74.
36. Takada T, Hayakawa H, Akiba E. Preparation and crystal structure refinement of Li4Mn5O12 by the Rietveld method. J Solid State Chem 1995;115:420–6.
37. Shi X, Zhang Z, Zhou D, Zhang L, Chen B, Yu L. Synthesis of Li+ adsorbent (H2TiO3) and its adsorption properties. Transactions of Nonferrous Metals Society of China 2013;23:253–9.
38. Chitrakar R, Makita Y, Ooi K, Sonoda A. Lithium recovery from salt lake brine by H 2 TiO 3. Dalton Transactions 2014;43:8933–9.
39. Zhang L, Zhou D, Yao Q, Zhou J. Preparation of H2TiO3-lithium adsorbent by the sol–gel process and its adsorption performance. Appl Surf Sci 2016;368:82–7.
40. Wang S, Li P, Cui W, Zhang H, Wang H, Zheng S, et al. Hydrothermal synthesis of lithium-enriched β-Li 2 TiO 3 with an ion-sieve application: Excellent lithium adsorption. RSC Adv 2016;6:102608–16.
41. Moazeni M, Hajipour H, Askari M, Nusheh M. Hydrothermal synthesis and characterization of titanium dioxide nanotubes as novel lithium adsorbents. Mater Res Bull 2015;61:70–5.
42. Ooi K, Miyai Y, Katoh S, Maeda H, Abe M. Topotactic lithium (1+) insertion to. lambda.-manganese dioxide in the aqueous phase. Langmuir 1989;5:150–7.
43. Shen X-M, Clearfield A. Phase transitions and ion exchange behavior of electrolytically prepared manganese dioxide. J Solid State Chem 1986;64:270–82.
44. Koyanaka H, Matsubaya O, Koyanaka Y, Hatta N. Quantitative correlation between Li absorption and H content in manganese oxide spinel λ-MnO2. Journal of Electroanalytical Chemistry 2003;559:77–81.

Preprints.org (www.preprints.org) | NOT PEER-REVIEWED | Posted: 6 February 2024 doi:10.20944/preprints202402.0329.v1

45. Koyanaka H, Matsubaya O, Koyanaka Y, Hatta N. Quantitative correlation between Li absorption and H content in manganese oxide spinel λ-MnO2. Journal of Electroanalytical Chemistry 2003;559:77–81.
46. Feng Q, Miyai Y, Kanoh H, Ooi K. Lithium (1+) extraction/insertion with spinel-type lithium manganese oxides. Characterization of redox-type and ion-exchange-type sites. Langmuir 1992;8:1861–7.
47. Ooi K, Miyai Y, Sakakihara J. Mechanism of lithium (1+) insertion in spinel-type manganese oxide. Redox and ion-exchange reactions. Langmuir 1991;7:1167–71.
48. Shen X-M, Clearfield A. Phase transitions and ion exchange behavior of electrolytically prepared manganese dioxide. J Solid State Chem 1986;64:270–82.
49. Hong H-J, Park I-S, Ryu T, Ryu J, Kim B-G, Chung K-S. Granulation of Li1.33Mn1.67O4 (LMO) through the use of cross-linked chitosan for the effective recovery of Li+ from seawater. Chemical Engineering Journal 2013;234:16–22. https://doi.org/https://doi.org/10.1016/j.cej.2013.08.060.
50. Ryu T, Haldorai Y, Rengaraj A, Shin J, Hong H-J, Lee G-W, et al. Recovery of Lithium Ions from Seawater Using a Continuous Flow Adsorption Column Packed with Granulated Chitosan–Lithium Manganese Oxide. Ind Eng Chem Res 2016;55:7218–25. https://doi.org/10.1021/acs.iecr.6b01632.
51. Ding W, Zhang J, Liu Y, Guo Y, Deng T, Yu X. Synthesis of granulated H4Mn5O12/chitosan with improved stability by a novel cross-linking strategy for lithium adsorption from aqueous solutions. Chemical Engineering Journal 2021;426:131689. https://doi.org/https://doi.org/10.1016/j.cej.2021.131689.
52. Yüksel Özşen A, Kahvecioğlu A. Adsorbent synthesis for the recovery of lithium water resources. Master of Science . Izmir Institute of Technology, 2022.
53. Wang H, Cui J, Li M, Guo Y, Deng T, Yu X. Selective recovery of lithium from geothermal water by EGDE cross-linked spherical CTS/LMO. Chemical Engineering Journal 2020;389:124410. https://doi.org/https://doi.org/10.1016/j.cej.2020.124410.
54. Xie Y, Zhang Y, Qin J, Samadiy M, Deng T. Synthesis of Spherical Composite CMC-LTO-EGDE-ME for Lithium Recovery from Geothermal Water. J Chem 2022;2022:6884947. https://doi.org/10.1155/2022/6884947.
55. Li X, Qi Y, Li Y, Zhang Y, He X, Wang Y. Novel magnetic beads based on sodium alginate gel crosslinked by zirconium (IV) and their effective removal for Pb2+ in aqueous solutions by using a batch and continuous systems. Bioresour Technol 2013;142:611–9.
56. Ozawa K. Lithium ion rechargeable batteries: materials, technology, and new applications. John Wiley & Sons; 2012.
57. Darul J, Nowicki W, Piszora P. Unusual compressional behavior of lithium–manganese oxides: a case study of Li4Mn5O12. The Journal of Physical Chemistry C 2012;116:17872–9.
58. Robinson DM, Go YB, Greenblatt M, Dismukes GC. Water oxidation by λ-MnO2: catalysis by the cubical Mn4O4 subcluster obtained by delithiation of spinel LiMn2O4. J Am Chem Soc 2010;132:11467–9.
59. Xiao G, Tong K, Zhou L, Xiao J, Sun S, Li P, et al. Adsorption and Desorption Behavior of Lithium Ion in Spherical PVC–MnO2 Ion Sieve. Ind Eng Chem Res 2012;51:10921–9. https://doi.org/10.1021/ie300087s.
60. Zhu G, Wang P, Qi P, Gao C. Adsorption and desorption properties of Li+ on PVC-H1.6Mn1.6O4 lithium ion-sieve membrane. Chemical Engineering Journal 2014;235:340–8. https://doi.org/https://doi.org/10.1016/j.cej.2013.09.068.
61. Yang Z, Li Y, Ma P. Synthesis of H2TiO3-PVC lithium-ion sieves via an antisolvent method and its adsorption performance. Ceram Int 2022;48:30127–34. https://doi.org/https://doi.org/10.1016/j.ceramint.2022.06.284.
62. Nisola GM, Limjuco LA, Vivas EL, Lawagon CP, Park MJ, Shon HK, et al. Macroporous flexible polyvinyl alcohol lithium adsorbent foam composite prepared via surfactant blending and cryo-desiccation. Chemical Engineering Journal 2015;280. https://doi.org/10.1016/j.cej.2015.05.107.
63. Limjuco LA, Nisola GM, Lawagon CP, Lee S-P, Seo JG, Kim H, et al. H2TiO3 composite adsorbent foam for efficient and continuous recovery of Li+ from liquid resources. Colloids Surf A Physicochem Eng Asp 2016;504:267–79. https://doi.org/https://doi.org/10.1016/j.colsurfa.2016.05.072.
64. Xiao J-L, Sun S-Y, Song X, Li P, Yu J-G. Lithium ion recovery from brine using granulated polyacrylamide–MnO2 ion-sieve. Chemical Engineering Journal 2015;279:659–66. https://doi.org/https://doi.org/10.1016/j.cej.2015.05.075.
65. Jia Q, Wang J, Guo R. Preparation and characterization of porous HMO/PAN composite adsorbent and its adsorption–desorption properties in brine. Journal of Porous Materials 2019;26:705–16. https://doi.org/10.1007/s10934-018-0662-8.
66. Lai X, Yijia Y, Chen Z, Peng J, Sun H, Zhong H. Adsorption-Desorption Properties of Granular EP/HMO Composite and Its Application in Lithium Recovery from Brine. Ind Eng Chem Res 2020;XXXX. https://doi.org/10.1021/acs.iecr.0c00668.
67. Zhou S, Guo X, Yan X, Chen Y, Lang W. Zr-doped titanium lithium ion sieve and EP-granulated composite: Superb adsorption and recycling performance. Particuology 2022;69:100–10. https://doi.org/https://doi.org/10.1016/j.partic.2021.12.002.

Preprints.org (www.preprints.org) | NOT PEER-REVIEWED | Posted: 6 February 2024 doi:10.20944/preprints202402.0329.v1

68. Liu J, Zhang Y, Miao Y, Yang Y, Li P. Alkaline Resins Enhancing Li+/H+ Ion Exchange for Lithium Recovery from Brines Using Granular Titanium-Type Lithium Ion-Sieves. Ind Eng Chem Res 2021;60:16457–68. https://doi.org/10.1021/acs.iecr.1c02361.
69. Zhang Y, Liu J, Yang Y, Lin S, Li P. Preparation of granular titanium-type lithium-ion sieves and recyclability assessment for lithium recovery from brines with different pH value. Sep Purif Technol 2021;267:118613. https://doi.org/https://doi.org/10.1016/j.seppur.2021.118613.
70. Hong H-J, Park I-S, Ryu J, Ryu T, Kim B-G, Chung K-S. Immobilization of hydrogen manganese oxide (HMO) on alpha-alumina bead (AAB) to effective recovery of Li+ from seawater. Chemical Engineering Journal 2015;271:71–8. https://doi.org/https://doi.org/10.1016/j.cej.2015.02.023.
71. Qian H, Huang S, Ba Z, Wang W, Yu F, Liang D, et al. Hto/cellulose aerogel for rapid and highly selective li+ recovery from seawater. Molecules 2021;26. https://doi.org/10.3390/molecules26134054.
72. Zhang X, Zheng X, Xu T, Zhang Y, Li G, Li Z. Synthesis of High Specific Surface Lithium-Ion Sieve Templated by Bacterial Cellulose for Selective Adsorption of Li. Molecules 2023;28:3191.
73. Liu C, Tao B, Wang Z, Wang D, Guo R, Chen L. Preparation and characterization of lithium ion sieves embedded in a hydroxyethyl cellulose cryogel for the continuous recovery of lithium from brine and seawater. Chem Eng Sci 2021;229:115984. https://doi.org/https://doi.org/10.1016/j.ces.2020.115984.
74. Li J, Luo Q, Dong M, Nie G, Liu Z, Wu Z. Synthesis of granulated Li/Al-LDHs adsorbent and application for recovery of Li from synthetic and real salt lake brines. Hydrometallurgy 2022;209:105828. https://doi.org/https://doi.org/10.1016/j.hydromet.2022.105828.
75. Koilraj P, Smith SM, Yu Q, Ulrich S, Sasaki K. Encapsulation of a powdery spinel-type Li+ ion sieve derived from biogenic manganese oxide in alginate beads. Powder Technol 2016;301:1201–7. https://doi.org/https://doi.org/10.1016/j.powtec.2016.08.009.
76. Park SH, Yan Y-Z, Kim J, Ha C-S, Lee SJ. Rapid and selective adsorption of Li+ from concentrated seawater using repulsive force of Al3+–crosslinked alginate composite incorporated with hydrogen manganese oxide. Hydrometallurgy 2022;208:105812. https://doi.org/https://doi.org/10.1016/j.hydromet.2021.105812.
77. Cheng M, Yao C, Su Y, Liu J, Xu L, Hou S. Synthesis of membrane-type graphene oxide immobilized manganese dioxide adsorbent and its adsorption behavior for lithium ion. Chemosphere 2021;279:130487. https://doi.org/https://doi.org/10.1016/j.chemosphere.2021.130487.
78. Han Y, Kim H, Park J. Millimeter-sized spherical ion-sieve foams with hierarchical pore structure for recovery of lithium from seawater. Chemical Engineering Journal 2012;210:482–9. https://doi.org/https://doi.org/10.1016/j.cej.2012.09.019.
79. Chen S, Chen Z, Wei Z, Hu J, Guo Y, Deng T. Titanium-based ion sieve with enhanced post-separation ability for high performance lithium recovery from geothermal water. Chemical Engineering Journal 2021;410:128320. https://doi.org/https://doi.org/10.1016/j.cej.2020.128320.
80. Udoetok I. Modified Biopolymer Sorbents for the Uptake of Naphthenic Acid Fraction Components (NAFCs) from Aqueous Solutions. Doctoral. University of Saskatchewan, 2018.
81. Ibrahim S, Riahi O, Said SM, Sabri MFM, Rozali S. Biopolymers From Crop Plants. Reference Module in Materials Science and Materials Engineering, 2019. https://doi.org/10.1016/b978-0-12-803581-8.11573-5.
82. Kaith BS, Mittal H, Bhatia JK, Kalia S. Polysaccharide Graft Copolymers – Synthesis, Properties and Applications. Biopolymers, John Wiley & Sons, Inc.; 2011, p. 35–57. https://doi.org/10.1002/9781118164792.ch2.
83. Pillai CKS, Paul W, Sharma CP. Chitin and chitosan polymers: Chemistry, solubility and fiber formation. Prog Polym Sci 2009;34:641–78. https://doi.org/10.1016/j.progpolymsci.2009.04.001.
84. Kumar MNVR. A review of chitin and chitosan applications. Elsevier Science B.V.; 2000.
85. Gu D, Sun W, Han G, Cui Q, Wang H. Lithium ion sieve synthesized via an improved solid state method and adsorption performance for West Taijinar Salt Lake brine. Chemical Engineering Journal 2018;350. https://doi.org/10.1016/j.cej.2018.05.191.
86. Zhang Q, Wu Q, Lin D, Yao S. Effect and mechanism of sodium chloride on the formation of chitosan–cellulose sulfate–tripolyphosphate crosslinked beads. Soft Matter 2013;9:10354–63. https://doi.org/10.1039/C3SM52051J.
87. Udoetok IA, Wilson LD, Headley J V. Self-Assembled and Cross-Linked Animal and Plant-Based Polysaccharides: Chitosan–Cellulose Composites and Their Anion Uptake Properties. ACS Appl Mater Interfaces 2016;8:33197–209. https://doi.org/10.1021/acsami.6b11504.
88. Udoetok IA, Wilson LD, Headley J V. "Pillaring Effects" in Cross-Linked Cellulose Biopolymers: A Study of Structure and Properties. Int J Polym Sci 2018;2018:6358254. https://doi.org/10.1155/2018/6358254.
89. Qiu X, Hu S. "Smart" Materials Based on Cellulose: A Review of the Preparations, Properties, and Applications. Materials 2013;6:738–81. https://doi.org/10.3390/ma6030738.
90. Yamazawa A, Iikura T, Shino A, Date Y, Kikuchi J. Solid-, Solution-, and Gas-state NMR Monitoring of 13C-Cellulose Degradation in an Anaerobic Microbial Ecosystem. Molecules 2013;18:9021–33. https://doi.org/10.3390/molecules18089021.

Preprints.org (www.preprints.org) | NOT PEER-REVIEWED | Posted: 6 February 2024 doi:10.20944/preprints202402.0329.v1

91. Boufi S, Alila S. Modified Cellulose Fibres as a Biosorbent for the Organic Pollutants 2011:483–524. https://doi.org/10.1002/9781118164792.ch17.
92. Zhang S, Li F-X, Yu J-Y. Kinetics of cellulose regeneration from cellulose-NaOH/thiourea/urea/H2O system. Cellulose Chemistry and Technology 2011;45:593.
93. Cai J, Zhang L. Rapid Dissolution of Cellulose in LiOH/Urea and NaOH/Urea Aqueous Solutions. Macromol Biosci 2005;5:539–48. https://doi.org/10.1002/mabi.200400222.
94. Qin X, Lu A, Zhang L. Effect of stirring conditions on cellulose dissolution in NaOH/urea aqueous solution at low temperature. J Appl Polym Sci 2012;126:E470–7. https://doi.org/10.1002/app.36992.
95. Zhou J, Zhang L. Solubility of Cellulose in NaOH/Urea Aqueous Solution. Polym J 2000;32:866–70. https://doi.org/10.1295/polymj.32.866.
96. Wang H, Gurau G, Rogers RD. Ionic liquid processing of cellulose. Chem Soc Rev 2012;41:1519. https://doi.org/10.1039/c2cs15311d.
97. Swatloski RP, Spear SK, Holbrey JD, Rogers RD. Dissolution of Cellose with Ionic Liquids. J Am Chem Soc 2002;124:4974–5. https://doi.org/10.1021/ja025790m.
98. Moulthrop JS, Swatloski RP, Moyna G, Rogers RD. High-resolution 13C NMR studies of cellulose and cellulose oligomers in ionic liquid solutions. Chemical Communications 2005:1557. https://doi.org/10.1039/b417745b.
99. Klemm D, Heublein B, Fink H-P, Bohn A. Cellulose: Fascinating Biopolymer and Sustainable Raw Material. Angewandte Chemie International Edition 2005;44:3358–93. https://doi.org/10.1002/anie.200460587.
100. Baysal K, Aroguz AZ, Adiguzel Z, Baysal BM. Chitosan/alginate crosslinked hydrogels: Preparation, characterization and application for cell growth purposes. Int J Biol Macromol 2013;59:342–8.
101. Udoetok IA, Faye O, Wilson LD. Adsorption of Phosphate Dianions by Hybrid Inorganic–Biopolymer Polyelectrolyte Complexes: Experimental and Computational Studies. ACS Appl Polym Mater 2020;2:899–910. https://doi.org/10.1021/acsapm.9b01123.
102. Hasnain MS, Jameel E, Mohanta B, Dhara AK, Alkahtani S, Nayak AK. Chapter 1 - Alginates: sources, structure, and properties. In: Nayak AK, Hasnain MS, editors. Alginates in Drug Delivery, Academic Press; 2020, p. 1–17. https://doi.org/https://doi.org/10.1016/B978-0-12-817640-5.00001-7.
103. Hasnain MS, Nayak AK. Alginates: versatile polymers in biomedical applications and therapeutics. CRC Press; 2019.
104. Yu Q, Morioka E, Sasaki K. Characterization of lithium ion sieve derived from biogenic Mn oxide. Microporous and Mesoporous Materials 2013;179:122–7.
105. Zhao B, Guo M, Qian F, Qian Z, Xu N, Wu Z, et al. Hydrothermal synthesis and adsorption behavior of H 4 Ti 5 O 12 nanorods along [100] as lithium ion-sieves. RSC Adv 2020;10:35153–63.
106. Mostafavi FS, Zaeim D. Agar-based edible films for food packaging applications - A review. Int J Biol Macromol 2020;159:1165–76. https://doi.org/https://doi.org/10.1016/j.ijbiomac.2020.05.123.
107. Martínez-Sanz M, Gómez-Mascaraque LG, Ballester AR, Martínez-Abad A, Brodkorb A, López-Rubio A. Production of unpurified agar-based extracts from red seaweed Gelidium sesquipedale by means of simplified extraction protocols. Algal Res 2019;38:101420.
108. Armisén R, Gaiatas F. 4 - Agar. In: Phillips GO, Williams PA, editors. Handbook of Hydrocolloids (Second Edition), Woodhead Publishing; 2009, p. 82–107. https://doi.org/https://doi.org/10.1533/9781845695873.82.
109. Schmidt ÉC, Dos Santos R, Horta PA, Maraschin M, Bouzon ZL. Effects of UVB radiation on the agarophyte Gracilaria domingensis (Rhodophyta, Gracilariales): changes in cell organization, growth and photosynthetic performance. Micron 2010;41:919–30.
110. Nieto MB, Akins M. Hydrocolloids in bakery fillings. Hydrocolloids in Food Processing 2010:67–107.
111. Nieto MB. Structure and function of polysaccharide gum-based edible films and coatings. Edible Films and Coatings for Food Applications 2009:57–112.
112. Han Y, Kim S, Kim H, Park J. Preparation of sizable and uniform-sized spherical ceramic foams: drop-in-oil and agar gelation. Journal of the American Ceramic Society 2011;94:2742–5.

Disclaimer/Publisher's Note: The statements, opinions and data contained in all publications are solely those of the individual author(s) and contributor(s) and not of MDPI and/or the editor(s). MDPI and/or the editor(s) disclaim responsibility for any injury to people or property resulting from any ideas, methods, instructions or products referred to in the content.